Electronic supplementary information

Molecular "backbone surgery" of electron-deficient heteroarenes based on dithienopyrrolobenzothiadiazole: conformation-dependent crystal structures and charge transport properties

Yuzhong Chen[1, 2], Zeng Wu[1, 2] , Zekun Chen[1], Shuixin Zhang[1], Wenhao Li[1], Yan Zhao[1], Yang Wang[1], and Yunqi Liu[1]*

[1] Department of Materials Science, State Key Laboratory of Molecular Engineering of Polymers, Fudan University, Shanghai 200438, China

E-mail: yangwang@fudan.edu.cn

[2] These authors contributed equally

Instruments and Measurements

Chemical synthesis and characterization

All commercially available solvents, reagents, and chemicals were purchased from Aldrich, TCI and several other reagent companies and used as received without further purification unless otherwise specified. All reactions and manipulations were carried out with the use of standard inert atmosphere and Schlenk techniques. Compound 1, compound 2, BTPO-c were synthesized according to the literature.[1, 2] ^{1}H NMR (400 MHz) and ^{13}C NMR (100 MHz) spectra were measured on a Varian Mercury Plus-400 spectrometer. The splitting patterns were designated as follows: s (singlet); d (doublet); t (triplet); m (multiplet). Deuterated chloroform was used as the solvent. The NMR chemical shifts were reported in ppm (parts per million) relative to the residual solvent peak at 7.26 ppm (chloroform) for the ^{1}H NMR spectroscopy and 77.2 ppm (chloroform) for the ^{13}C NMR spectroscopy. The MALDI−TOF mass spectra were measured by a Bruker autoflex maX MALDI-TOF mass spectrometer.

TGA measurements

TGA measurement was carried out on Mettler STARe (TA Instrument) with a heating ramp of 10 ºC min^{-1} under nitrogen flow.

Optical characterizations

UV-Vis absorption spectra were acquired from PerkinElmer Lambda 750 spectrophotometer. All film samples were spin-cast on glass substrates. All the solution of small molecules were measured with a concentration of 0.02 mg/mL in chloroform.

Electrochemical characterizations

Cyclic voltammetry (CV) measurements of films were performed under argon atmosphere using a CHI760E voltammetric analyzer with 0.1 M tetra-n-butylammonium hexafluorophosphate (nBu$_4$NPF$_6$) in acetonitrile as the supporting electrolyte. A platinum disk working electrode, a platinum wire counter electrode, and a Ag/AgCl reference electrode were employed. The scanning rate was 0.1 V s^{-1} . Films were drop-casted from chloroform solutions of organic molecules on a Pt working electrode (2 mm in diameter). The supporting electrolyte solution was thoroughly purged with argon before all CV measurements. For calibration, the redox potential of ferrocene/ferrocenium (Fc/Fc$^+$) was measured under the same conditions. It was assumed that the redox potential of Fc/Fc$^+$ has an absolute energy level of -4.80 eV to a vacuum. The HOMO energy levels were determined by E_{HOMO} = - [q (E_{re} – $E_{ferrocene}$) + 4.8 eV], while the LUMO energy levels were determined by E_{LUMO} = - [q (E_{ox} – $E_{ferrocene}$) + 4.8 eV].

DFT calculations

The geometry optimizations of BTPO-c, BTPO-z and BTPO-l were performed on Gaussian 16 Rev. B.01. on B3LYP/6-31G (d) level, where the side chains are simplified with ethyl or methoxyl (if not specified) and bottom side chains are replaced with isobutyl.[3]

According to first-principles quantum mechanics calculations and Marcus theory, the electron transfer rate (k) is described by the Marcus-Hush equation as given in Equation S1,[4, 5]

$$k = \frac{V^2}{\hbar}\left(\frac{\pi}{\lambda_e k_B T}\right)^{1/2} exp\left(-\frac{\lambda_e}{4k_B T}\right) \quad \text{(S1)}$$

where V is the electronic coupling between adjacent molecules in dimer extracted from the crystal structure, λ_e is the electronic reorganization energy, T is the temperature and k_B is the Boltzmann constant. Here, only two parameters in Equations S1, V and λ_e, are unknown for a crystal structure, and both can be determined from the first-principles calculations.

Electronic coupling V is calculated by Equation (S2)

$$V = (J_{ij} - S_{ij} \times (\varepsilon_i + \varepsilon_j)/2)/(1 - S_{ij}^2) \quad \text{(S2)}$$

For electron mobility calculations the fragment LUMO are considered. Therefore, in Equation S2, J_{ij} stands for the charge transfer integral between LUMO of molecule i and LUMO of molecule j, S_{ij} stands for spatial overlap integral between LUMO of molecule i and LUMO of molecule j, ε_i and ε_j are the energy of the charge when it is localized at molecules, i and j, respectively, known as the site energy. The relative calculations are performed with the PW91/TZP of DFT implemented in the Amsterdam density functional (ADF) program.[6, 7]

The calculation methods for λ_e are provided in Equations S3,[8]

$$\lambda_e = E_0^* - E_0 + E_{-1}^* - E_{-1} \quad \text{(S3)}$$

where E_0 and E_{-1} represent the energies of the neutral and anionic species with negative charge of 1 in their lowest-energy geometries, respectively while E_0^* and E_{-1}^* are the energies of the neutral and anionic states with negative charge of 1 with the geometries of the anionic with negative charge of 1 and neutral species. Before the single point energy calculation, the geometry optimizations of BTPO-c, BTPO-z and BTPO-l were

performed on Gaussian 16 Rev. B.01. on B3LYP/6-311G (d, p) level, where the side chains are simplified with methyl or methoxyl (if not specified). Then the corresponding single-point energy is calculated under the same condition.

According to hopping mode, for perfect single crystals, the hopping electron mobility (μ_e) is calculated by using the Einstein relation in Equation (S4),[9]

$$\mu_e = \frac{e}{k_B T} D \qquad \text{(S4)}$$

where e is the electronic charge and D is the diffusion coefficient that is calculated from Equation (S5),[10]

$$D = \frac{1}{2}\sum_i r_i^2 k_i P_i cos^2(\varphi - \theta_i) cos^2\gamma_i \qquad \text{(S5)}$$

where i stands for the various types of dimers exist around one chosen monomer extracted from single crystals, r_i is the ith hopping distance, θ_i is the ith angle between the hopping path of the dimer and the reference axis, γ_i is the ith angle between the adjacent molecule and the plane of interest, k_i is the charge-hopping rate, φ is the orientation angle of the transport channel relative to the reference axis and P_i is the ith hopping probability, which is calculated by Equation (S6),[11]

$$P_i = \frac{k_i}{\sum_i k_i} \qquad \text{(S6)}$$

Therefore, electron mobility (μ_e) can be given as Equation (S7),[12]

$$\mu_e = \frac{e}{2k_B T}\sum_i r_i^2 k_i P_i cos^2(\varphi - \theta_i) cos^2\gamma_i \qquad \text{(S7)}$$

Binding Energy (ΔE) is defined as the energy difference between the complex and two monomers as shown in Equation S8,[13]

$$\Delta E = E_{dimer} - 2E_{monmer} \qquad \text{(S8)}$$

Here, the energy calculations were performed on ground state with the function B3LYP and the basis set at def2SVP.

Finally, the values of average π–π stacking distance (d) are directly taken by the molecular packing architecture in the organic crystal using Mercury software. And the hopping distance (r_i) is defined by the distance between two molecular centroids in one dimer, which combined with θ_i and γ_i can also be directly measured in Mercury software. [14]

AFM analysis

Atomic force microscopy (Park XE7) with tapping-mode was used to measure the surface morphology of films and the thickness of single crystals. All film samples were spin-cast on glass substrates according to devices fabrication conditions.

GIWAXS characterization

Grazing incidence X-ray diffraction (Shanghai Synchrotron Radiation Facility, Beamline 15U) was used to characterize the film texture of the organic semiconductor layers.[15]

Single crystal analysis

The single crystals of BTPO-c, BTPO-z and BTPO-l for X-ray crystallography analysis were grown by using the vapor diffusion strategy based on a mixture of chlorobenzene and methanol. A mother solution was prepared from ~3 mg molecule in ~1mL chlorobenzene in a 4 mL vial, which was capped with a piece of aluminum foil with several holes punched using a needle in the middle. The 4 mL vial was then placed in

a 20 mL vial containing ~5 mL methanol. The 20 mL vial was then tightly sealed, and left standing for 2-4 days to give out corresponding single crystals for measurements.[16-18]

For BTPO-l and BTPO-z, the single-crystal X-ray diffraction data were collected from shock-cooled single crystals at 193 K and 150 K on a D8 VENTURE METLAJET with a Liquid X-ray Source using GaKα radiation (λ = 1.34139 Å) and CuKα radiation (λ = 1.54178 Å) as monochromator and a Bruker PHOTON III detector. All data were integrated with SAINT and a multi-scan absorption correction using SADABS was applied.

For BTPO-c, a suitable crystal was selected and measured on a synchrotron radiation diffractometer (λ = 0.68878 Å). The crystal of BTPO-c was kept at 273.15 K during data collection.

The structure was solved by direct methods using SHELXT and refined by full-matrix least-squares methods against F2 by SHELXL-2019/2. All non-hydrogen atoms were refined with anisotropic displacement parameters. All hydrogen atoms were refined isotropic on calculated positions using a riding model with their U_{iso} values constrained to 1.5 times the U_{eq} of their pivot atoms for terminal sp^3 carbon atoms and 1.2 times for all other carbon atoms. Crystallographic data for the structures reported in this paper have been deposited with the Cambridge Crystallographic Data Centre. CCDC 2244244, 2254615 and 2255233 contain the supplementary crystallographic data for BTPO-l, BTPO-z and BTPO-c, respectively. These data can be obtained free of charge from The Cambridge Crystallographic Data Centre via www.ccdc.cam.ac.uk/

structures. This report and the CIF file were generated using FinalCif.

Fabrication of single-crystal devices of OFET

The bottom gate/ top contact (BGTC) OFET devices based on the single crystals of BTPO-c, BTPO-z and BTPO-l were fabricated with a "gold-stripes-stick" method.[19] A Si/SiO_2 wafer was used as substrate and work as gate electrode and dielectric. The substrate was firstly cleaned with piranha solution, and followed by sonication in deionized water and ethanol, respectively. After that, the octadecyltrichlorosilane (OTS) gas-phase modification process was conducted in 120 ℃ for 3 hours, followed by sonication cleaning in *n*-hexane, isopropanol and chloroform respectively. The single crystal was obtained by drop casting 20 μL 0.5 mg/mL BTPO-c, BTPO-z or BTPO-l o-dichlorobenzene solution on the OTS-modified substrate and placed in an undisturbed environment. Finally, two 100 nm Au layers were separately transferred onto the single crystal to work as source and drain electrodes and the channel width and length were measured with optical microscope. Optical microscope (Nikon LV100ND) with polarized mode was used to observe the single crystal optical properties.

Fabrication of Thin-Film OFETs

The TG/BC OFET devices based on films of the three molecules BTPO-c, BTPO-z or BTPO-l were fabricated with spin-coating process. The glass pieces were used as substrate after cleaned by sonication in deionized water, acetone and isopropanol for 10 minutes, respectively. A layer of 30 nm Au was deposited on the cleaned glass pieces via a thermal evaporation process to work as source and drain electrodes. The channel was formed with assistance of a metal shadow mask. The organic semiconductor layers

were prepared by spin-coating process, followed by an annealing process at 90 ℃ for 30 minutes. During this process, the chloroform solution of three molecules (40 μL, 5 mg/mL) was spinned firstly at 1500 rpm for 60 seconds. Then 60 μL PMMA butylacetate solution (80 mg/mL) was spinned in 1500 rpm for 60 seconds to work as the dielectric layers. Finally, an Ag layer of 100 nm was deposited on the dielectric layer with thermal evaporation process to work as gate electrode. The entire processing process, except for cleaning the glass pieces, were carried out in the glove box with nitrogen atmosphere.

Measurement of OFET devices

The OFET devices of both films and single crystals were measured in glove box with nitrogen atmosphere. Primarius Technologies FS-pro PDA semiconductor characterization system was utilized to measure the transfer and output curves of OFET. The saturation charge-carrier mobility (μ) was calculated according to the equation: $I_{DS} = (W\mu C_i/2L)(V_G-V_{th})^2$, where the I_{DS} is the source-drain current, W and L are the channel width and length of OFET, C_i is the capacitance per unit area of dielectric and C_i (PMMA) = 3 nF/cm^2 , C_i (SiO_2) = 11.5 nF/cm^2 in this work according to our measure, V_G and V_{th} are the gate voltage and threshold, respectively.

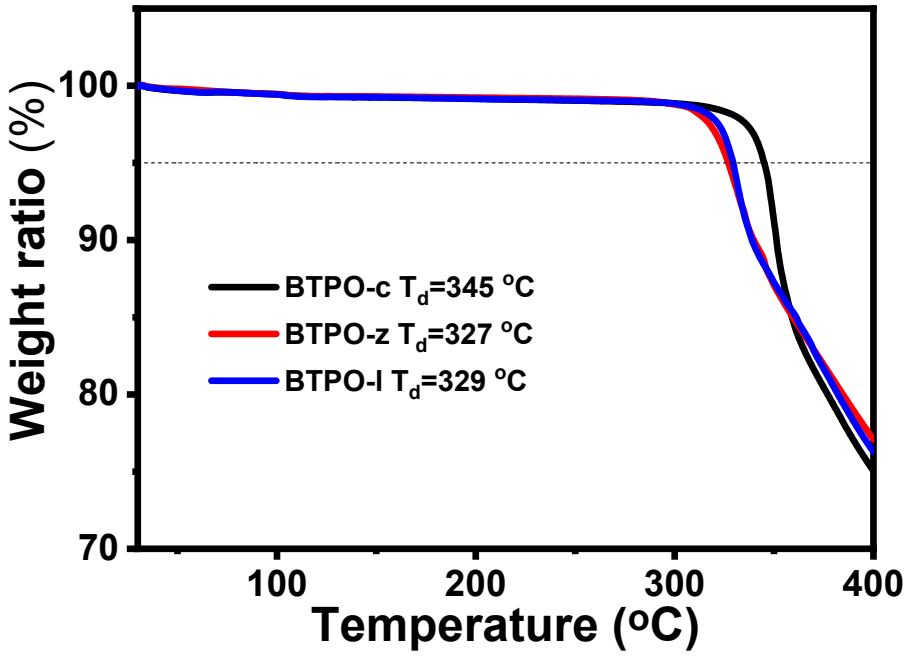

Figure S1. Thermogravimetric analysis (TGA) curves of BTPO-c, BTPO-z and BTPO-l.

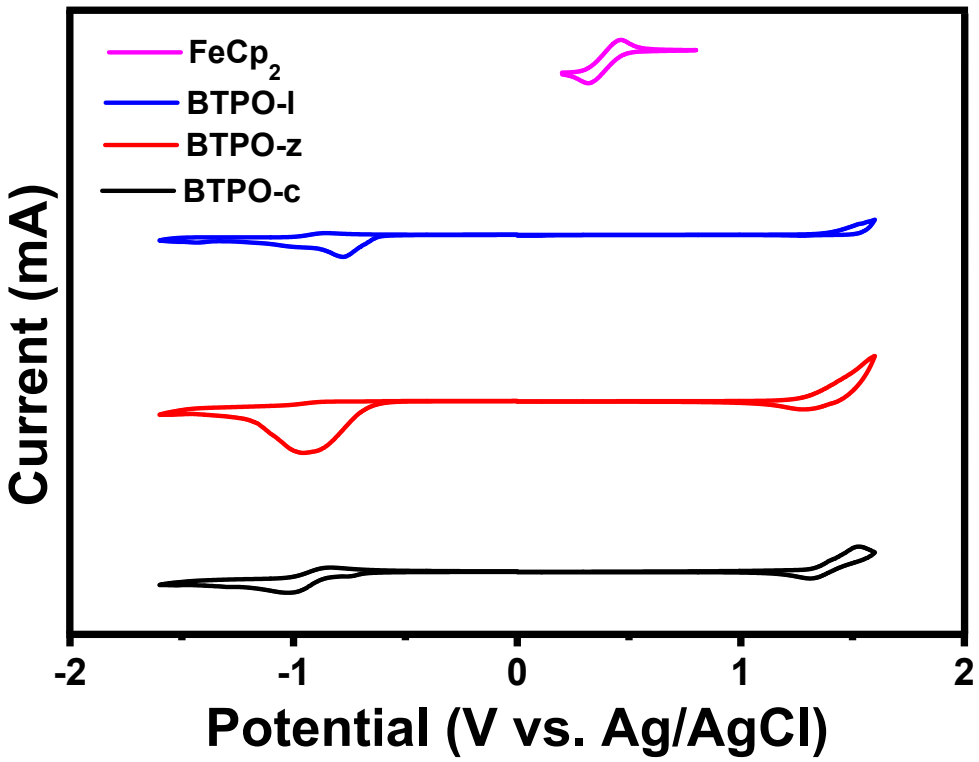

Figure S2. The CV plots of BTPO-c, BTPO-z and BTPO-l.

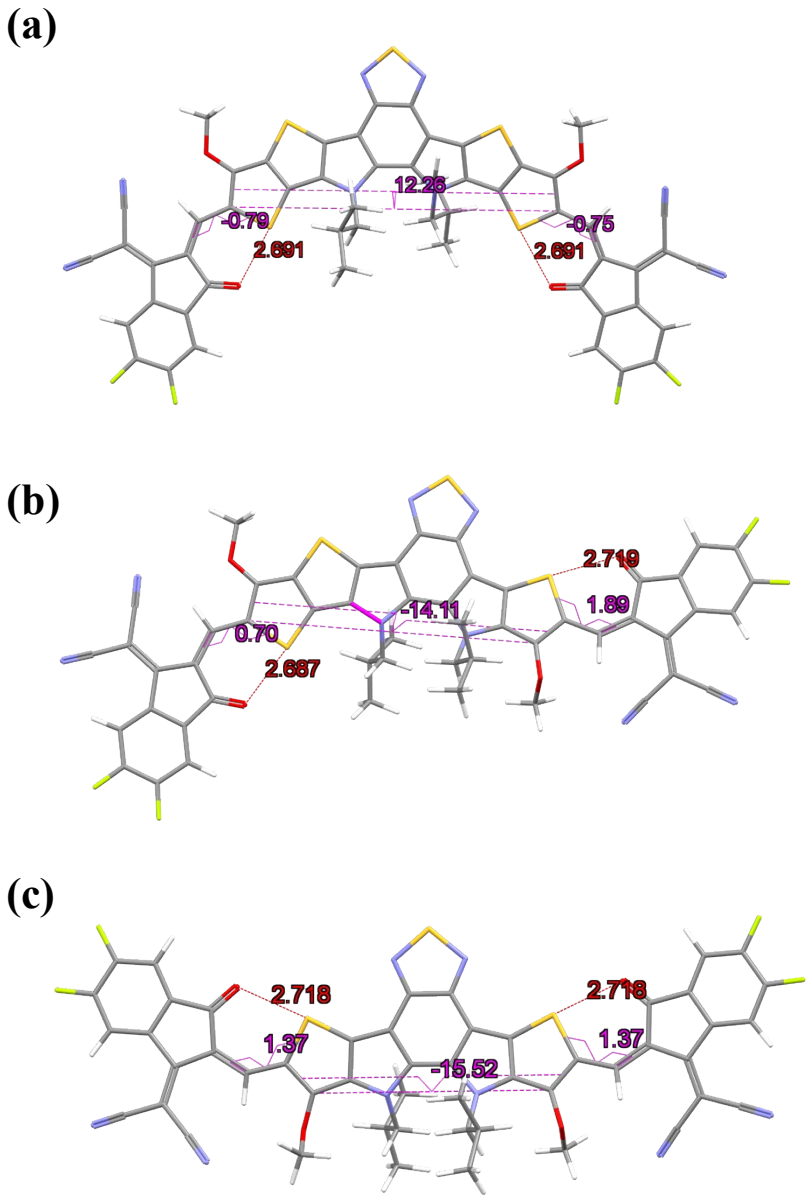

Figure S3. The optimized molecular geometries of (a) BTPO-c, (b) BTPO-z, and (c) BTPO-l calculated on Gaussian 16 Rev. B.01. on B3LYP/6-31G(d) level (the side chains are simplified with methyl or isobutyl).

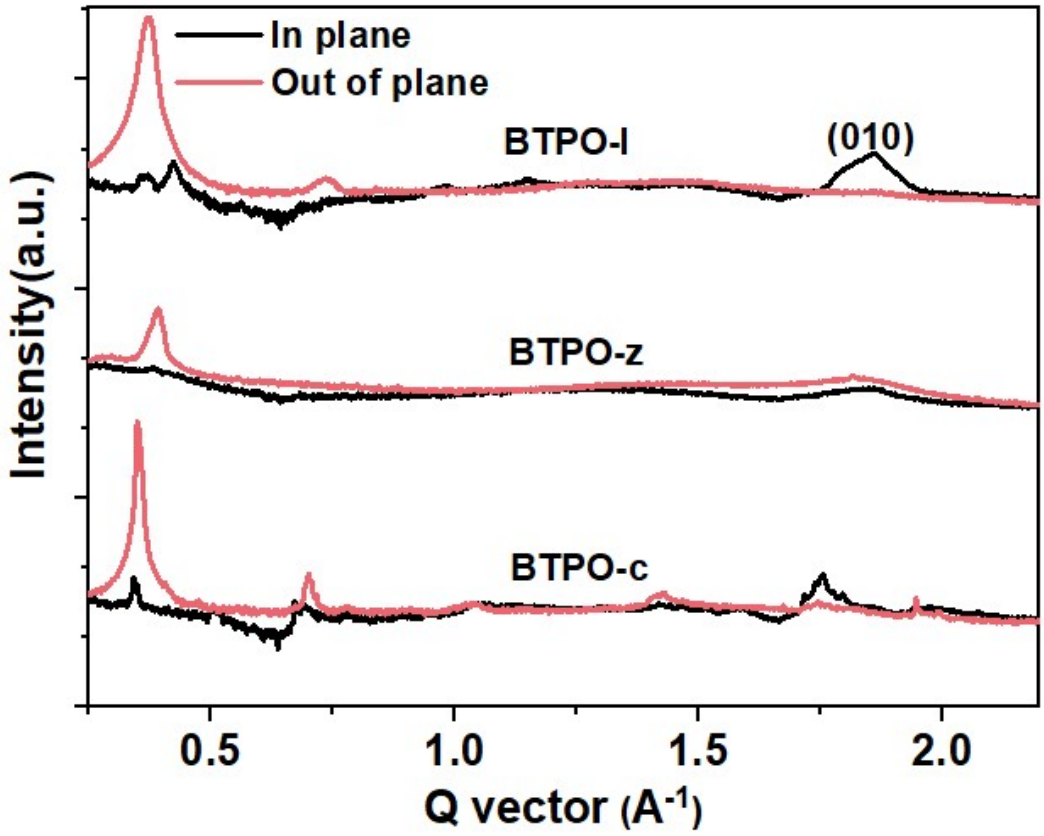

Figure S4. The corresponding in-plane and out-of-plane 1D GIWAXS profiles.

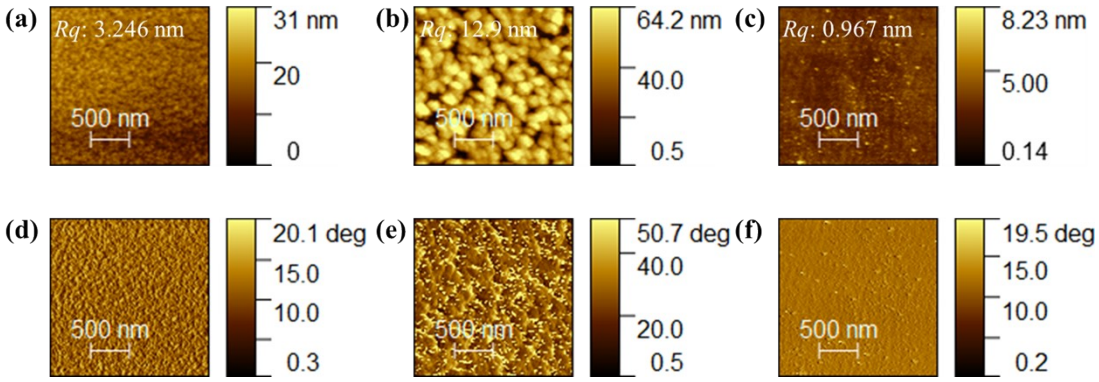

Figure S5. (a)~(c) The AFM topography images of BTPO-c, BTPO-z, and BTPO-l, respectively; (d)~(f) The AFM phase images of BTPO-c, BTPO-z, and BTPO-l, respectively.

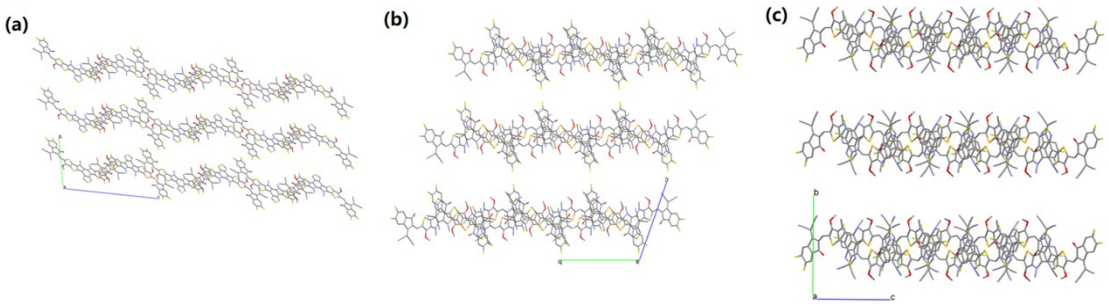

Figure S6. Single-crystal packing structures of BTPO-c (a), BTPO-z (b) and BTPO-l (c) in the [100] direction.

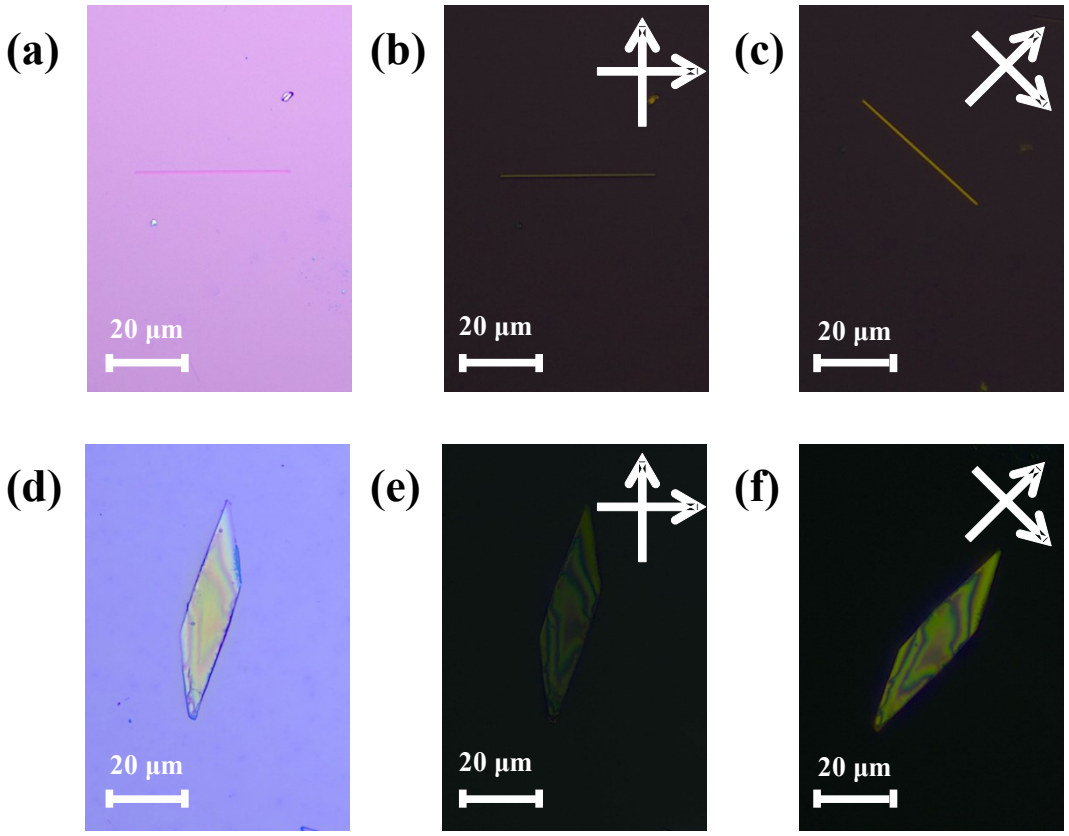

Figure S7. Optical microscopy images (a), (d) and polarized optical microscopy images (b-c), (e-f) of single crystals of BTPO-c and BTPO-z, respectively.

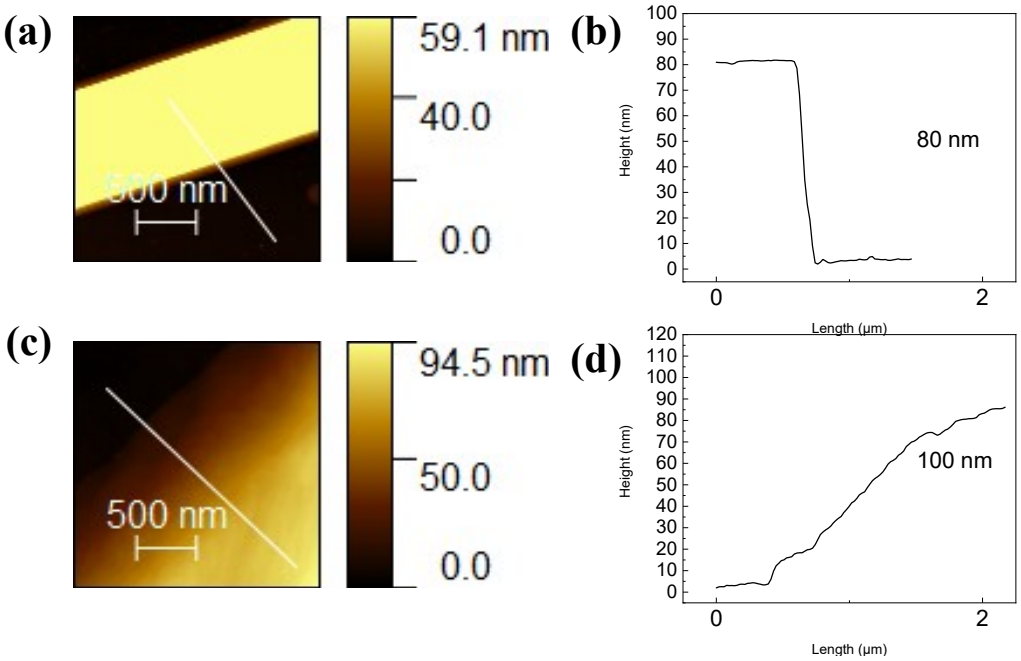

Figure S8. AFM images (a), (c) and corresponding height (b), (d) of single crystals of BTPO-c and BTPO-z, respectively.

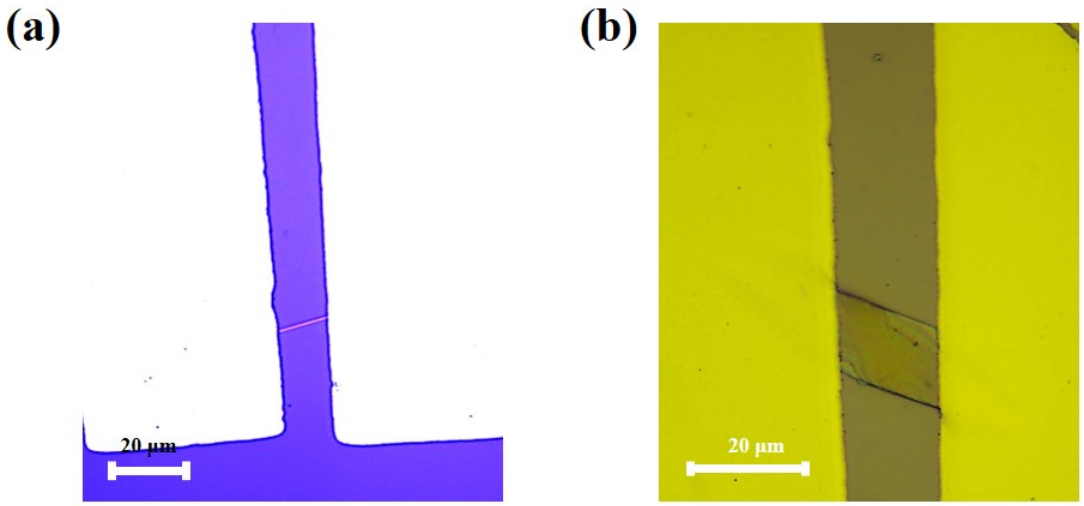

Figure S9. Optical microscopy images of OFETs based on single crystals of (a) BTPO-c and (b) BTPO-z, respectively.

Table S1. DFT calculation results of energy levels and dipole moment of BTPO-c, BTPO-z and BTPO-l.

Molecule	BTPO-c	BTPO-z	BTPO-l
HOMO	-5.59 eV	-5.67 eV	-5.84 eV
LUMO	-3.38 eV	-3.48 eV	-3.62 eV
Dipole moment (Debye)	3.66	1.25	1.49

Table S2. Morphological parameters obtained from GIWAXS.

Samples	In plane (010)				Out pf plane (100)			
	location ($Å^{-1}$)	π-spacing[a)] (Å)	FWHM (Å)	CL[b)] (Å)	location ($Å^{-1}$)	d-spacing[a)] (Å)	FWHM (Å)	CL[b)] (Å)
BTPO-c	1.75	3.59	0.031	182.4	0.350	18.0	0.0098	577.0
BTPO-z	1.86	3.38	0.181	31.2	0.389	16.2	0.0249	227.1
BTPO-l	1.85	3.40	0.103	54.9	0.370	17.0	0.0246	229.9

[a)] Obtained by the equation of $d = 2\pi/q$, in which q is the corresponding x-coordinate of diffraction peak; [b)] Calculated using the equation: $CL = 2\pi K/w$, in which w is the full width at half maxima and K is a form factor (0.9 here).

Table S3. The OFET performances based on the films of BTPO-c, BTPO-z and BTPO-l.

Semiconductor	$\mu_{e\ max}$ ($cm^2\ V^{-1}\ s^{-1}$)	$\mu_{e\ average}$[a)] ($cm^2\ V^{-1}\ s^{-1}$)	V_{th} (V)	I_{on}/I_{off} ratio
BTPO-c	0.1	0.08	12	~10^2
BTPO-z	0.006	0.004	-5	~10^3
BTPO-l	0.02	0.01	6	~10^4

[a)]The average values of the electron mobilities collected from at least 10 devices.

Table S4. Crystallographic data for BTPO-c, BTPO-z and BTPO-l.

Compound	BTPO-c	BTPO-z	BTPO-l
Moiety formula	$C_{82}H_{86}N_8O_4S_5F_4$	$C_{75}H_{76}N_8O_4S_4F_4$	$C_{68}H_{66}N_8O_4S_3F_4$
Formula weight	1483.88	1357.67	1231.46
Temperature (K)	273	120	193
Wavelength (Å)	0.69	1.54	1.34
Crystal system	triclinic	triclinic	monoclinic
Space group	P -1	P-1	Pc
a (Å)	10.9852(10)	13.8827(7)	15.304(2)
b (Å)	14.5835(12)	16.3666(9)	16.518(3)
c (Å)	26.719(3)	18.0937(11)	12.812(2)
α (º)	98.535(2)	103.449(5)	90
β (º)	98.131(2)	104.665(4)	104.845(10)
γ (º)	105.597(2)	107.099(4)	90
Volume ($Å^3$)	4002.7(6)	3585.7(4)	3130.8(9)
Density (g/cm^3)	1.231	1.257	1.306
Z	2	2	2
F(000)	1564.0	1428.0	1292.0
μ (mm^{-1})	0.192	1.744	1.069
h, k, lmax	10, 11, 25	15, 18, 20	17, 18, 14
R(reflections)	0.0903(5126)	0.1082(5734)	0.1793(2693)
wR2(reflections)	0.2778(6844)	0.2834(10905)	0.4396(8016)

S	1.058	1.046	1.176
packing coefficient[a)]	62.9	64.2	66.6

[a)]Determined with the PLATON program, using the VOID command.

Table S5. Calculated values of electronic reorganization energy, π–π stacking distance,

binding energy and charge transfer parameters for BTPO-c, BTPO-z and BTPO-l.

Molecule	**BTPO-c**			**BTPO-z**			**BTPO-l**	
Electronic reorganization energies (λ_e, eV)	0.1977			0.2052			0.2178	
dimer	c1	c2	c3	s1	s2	s3	w1	w2
Average π–π stacking distance (d, Å)	3.51	3.38	3.21	3.53	3.42	3.52	3.51	3.30
Binding Energy (ΔE, eV)	2.00	1.06	1.95	2.09	1.20	1.45	1.93	0.90
Electronic coupling (V, meV)	11.5	42.4	13.6	2.1	42.6	7.3	37.8	14.9
Effective charge transfer rate (k, ×10^{13} s^{-1})	0.149	2.025	0.210	0.005	1.953	0.057	1.426	0.222
Hoping distance (r, Å)	14.9	19.6	13.1	9.2	18.1	19.5	10.3	22.3
Hopping angle (θ, °)	347.6	129.1	161.1	118.3	79.1 /259.1	278.9	126.2 /306.2	81.5 /261.5
Hopping angle (γ, °)	21.1	0.6	0.6	17.4	0	17.4	52.1	0
Predicted μ_e (cm^2 V^{-1} s^{-1})	0.015~6.362			0.0003~5.765			0.053~0.492	

Materials and synthesis

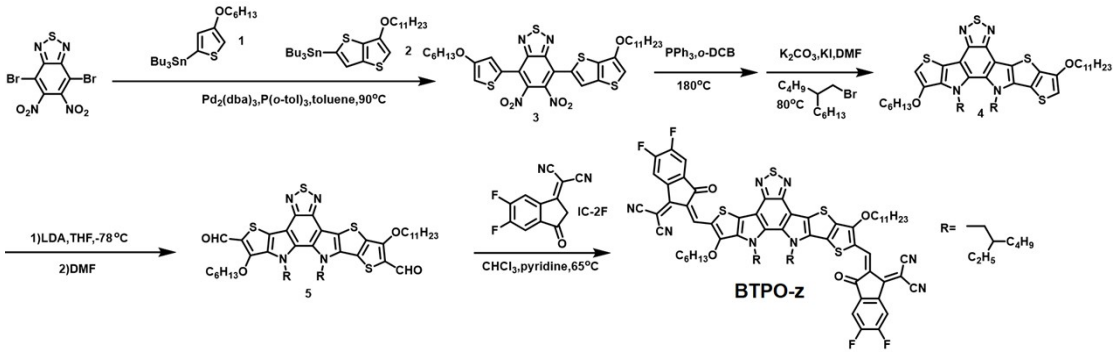

Scheme S1. The synthetic routes of **BTPO-z**.

Synthesis of compound **3**

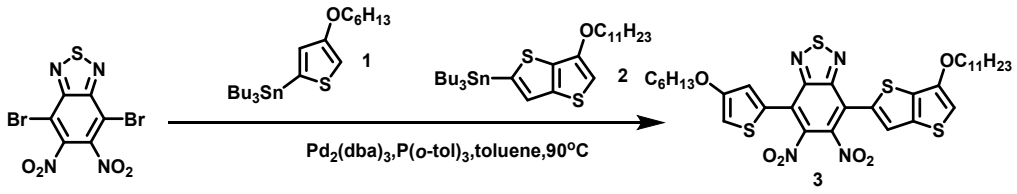

To a solution of 4,7-dibromo-5,6-dinitrobenzo[c][1,2,5]thiadiazole (200.0 mg, 0.521 mmol), $Pd_2(dba)_3$ (23.8 mg, 0.0260 mmol) and P(*o*-tol)$_3$ (63.4 mg, 0.208 mmol) in toluene (10 mL), compound **1** (259.9 mg, 0.625 mmol) and compound **2** (374.8 mg, 0.625 mmol) were added under N_2. The reaction mixture was stirred for 12 hours at 90 ^oC. Then, the reaction mixture was cooled to room temperature and poured into an aqueous potassium fluoride. The mixture was extracted with ethyl acetate for three times. The combined organic phase was washed with water followed by brine. Then the solution was dried over Na_2SO_4 and concentrated under reduced pressure. The residue was purified by flash column chromatography (eluent: *n*-hexane: CH_2Cl_2= 3:1, v/v) to get the product as dark red oil (125.0 mg, 34%).^{1}H NMR (400 MHz, $CDCl_3$, ppm): δ= 7.59 (s, 1H), 7.19 (d, 1H, *J*= 4.0 Hz), 6.65 (d, 1H, *J*= 4.0 Hz), 6.41 (s, 1H), 4.09 (t, 2H, *J*= 6.0 Hz), 3.99 (t, 2H, *J*= 6.0 Hz), 1.86-1.78 (m, 4H), 1.49-1.46 (m, 4H),

1.38-1.28 (m, 18H), 0.95-0.87 (m, 6H); ^{13}C NMR (100 MHz, $CDCl_3$, ppm): δ= 158.1, 152.1, 149.9, 141.8, 141.6, 137.2, 134.8, 130.8, 128.2, 124.2, 123.2, 121.3, 104.0, 101.2, 71.0, 70.7, 32.1, 31.7, 29.8, 29.7, 29.5, 29.5, 29.3, 26.2, 25.8, 22.8, 22.7, 14.3, 14.2. MALDI-TOF MS: calcd for $C_{33}H_{40}N_4O_6S_4$, 716.1831; found, 716.2074.

Synthesis of compound **4**

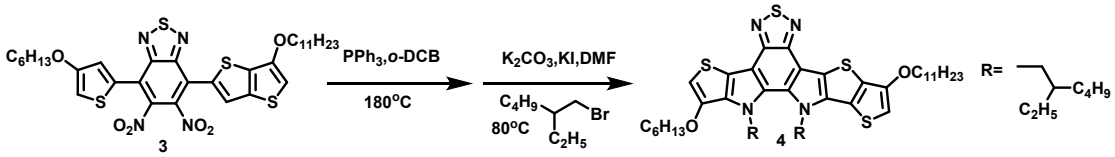

Compound **3** (30.0 mg, 0.0419 mmol) and PPh_3 (110.7 mg, 0.419 mmol) were dissolved in the 1,2-dichlorobenzene (*o*-DCB, 10 mL) under nitrogen. After being heated at 180 °C for 3 hrs, the solvent was removed to get the crude product.

The red residue was mixed with 3-(bromomethyl)heptane (194.2 mg, 1.01 mmol), potassium carbonate (115.8 mg, 0.838 mmol) and potassium iodide (166.9 mg, 1.01 mmol) in DMF (10 mL) under N_2. The mixture was refluxed at 80 °C overnight. After cooled down to room temperature, the residue was poured into water and extracted with ethyl acetate three times. The combined organic phase was washed with water followed by brine. Then the solution was dried over Na_2SO_4 and concentrated under reduced pressure. The residue was purified by flash column chromatography (eluent: *n*-hexane: CH_2Cl_2= 4:1, v/v) to get the product as orange oil (15.0 mg, 41%). ^{1}H NMR (400 MHz, $CDCl_3$, ppm): δ= 6.32 (s, 1H), 6.29 (s, 1H), 4.60-4.53 (m, 4H), 4.18-4.14 (m, 4H), 2.07-1.85 (m, 6H), 1.52-1.48 (m, 4H), 1.41-1.25 (m, 20H), 0.97-0.83 (m, 20H), 0.64-0.59 (m,12H); ^{13}C NMR (100 MHz, $CDCl_3$, ppm): δ= 151.4, 147.8, 147.6, 144.8, 136.9, 134.8, 133.6, 132.7, 132.0, 122.8, 122.4, 120.4, 111.9, 110.7, 98.2, 96.0, 71.0, 70.7,

55.1, 53.5, 40.4, 40.2, 32.1, 31.8, 29.9, 29.9, 29.8, 29.8, 29.6, 29.4, 26.3, 26.1, 23.3, 23.0, 22.9, 22.9, 14.3, 14.3, 14.0, 13.9. MALDI-TOF MS: calcd for $C_{49}H_{72}N_4O_2S_4$, 876.4538; found, 876.5045.

Synthesis of compound **5**

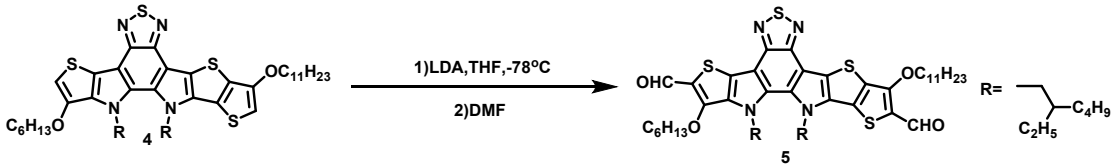

To a solution of compound **4** (146.0 mg, 0.0657 mmol) in THF (10 mL), 2.0 M lithium diisopropylamide in hexane (0.67 mL, 1.33 mmol) was added dropwise slowly at −78 °C under N_2. The mixture was stirred at −78 °C for 1 h, and then anhydrous DMF (0.67 mL) was added. The mixture was stirred overnight at room temperature. Brine was added and the mixture was extracted with ethyl acetate for three times. The combined organic phase was washed with water followed by brine. Then the solution was dried over Na_2SO_4 and concentrated under reduced pressure. The residue was purified by flash column chromatography (eluent: CH_2Cl_2) to get the product as orange solid (150.0 mg, 96 %).^{1}H NMR (400 MHz, $CDCl_3$, ppm): δ= 10.19 (s, 1H), 10.10 (s, 1H), 4.69 (t, 2H, *J*= 6.0 Hz), 4.60-4.49 (m, 6H), 2.08-1.88 (m, 6H), 1.58-1.55 (m, 4H), 1.42-1.28 (m, 20H), 0.96-0.86 (m, 20H), 0.67-0.61 (m, 12H); ^{13}C NMR (100 MHz, $CDCl_3$, ppm): δ= 181.5, 181.5, 158.9, 150.3, 147.8, 147.6, 137.1, 136.6, 135.8, 132.9, 130.1, 129.9, 128.2, 128.1, 127.6, 122.2, 113.0, 112.0, 77.7, 73.5, 55.0, 54.2, 40.7, 40.5, 32.1, 31.7, 30.3, 30.1, 29.8, 29.8, 29.7, 29.5, 29.5, 27.7, 26.0, 25.8, 23.2, 22.9, 22.8, 14.3, 14.2, 13.9, 13.9. MALDI-TOF MS: calcd for $C_{51}H_{72}N_4O_4S_4$, 932.4436; found, 932.4975.

Synthesis of **BTPO-z**

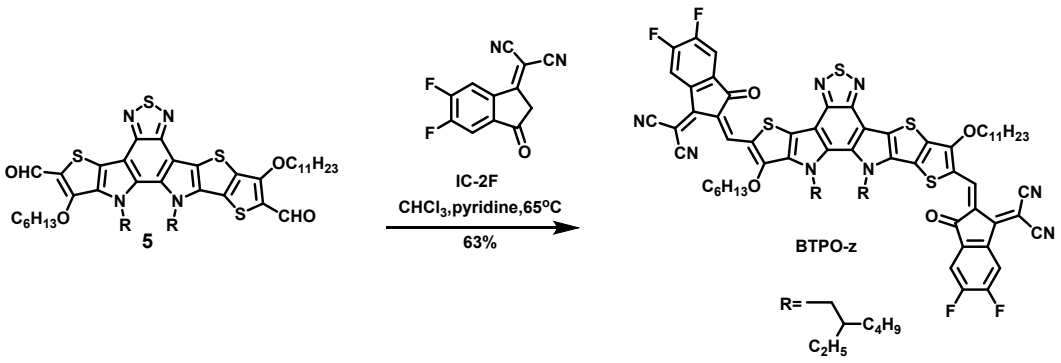

To a solution of compound **5** (70.0 mg, 0.0750 mmol) and 2-(5, 6-difluoro-3-oxo-2,3-dihydro-1*H*-inden-1-ylidene) malononitrile (**IC-2F**) (103.6 mg, 0.450 mmol) in dry $CHCl_3$ (10 mL) was added pyridine (1 mL) under N_2. The mixture was refluxed for 16 hours and then allowed to cool to room temperature, then the mixture was poured into CH_3OH (100 mL) and filtered, the residue left in filter paper was dissolved by $CHCl_3$. After removing the solvent, the residue was purified using column chromatography on silica gel (eluent: *n*-hexane: CH_2Cl_2= 1:1 , v/v), yielding a dark purple solid (72.0 mg, 63%).^{1}H NMR (400 MHz, $CDCl_3$, ppm): δ= 9.31 (s, 1H), 9.24 (s, 1H), 8.56-8.47 (m, 2H), 7.70-7.62 (m, 2H), 4.79-4.76 (m, 4H), 4.59-4.58 (m, 2H), 4.44 (t, 2H, *J*= 8.0 Hz), 2.12-1.98 (m, 6H), 1.42-1.28 (m, 24H), 1.03-0.67 (m, 32H); ^{13}C NMR (100 MHz, $CDCl_3$, ppm): δ= 186.8, 186.2, 162.6, 159.1, 158.7, 156.3, 155.6, 153.6, 147.7, 147.6, 138.5, 137.0, 136.7, 134.7, 134.5, 133.7, 131.6, 128.9, 127.9, 120.3, 120.2, 118.2, 115.0, 114.8, 114.6, 113.7, 79.4, 74.4, 55.4, 54.9, 40.9, 40.4, 32.2, 31.9, 30.1, 29.9, 29.9, 29.9, 29.8, 29.6, 29.5, 28.1, 27.6, 26.0, 25.8, 23.5, 23.1, 22.9, 22.9, 14.4, 14.3, 14.0, 13.9, 10.3, 10.1. MALDI-TOF MS: calcd for $C_{75}H_{76}F_4N_8O_4S_4$, 1356.4808; found, 1356.4274.

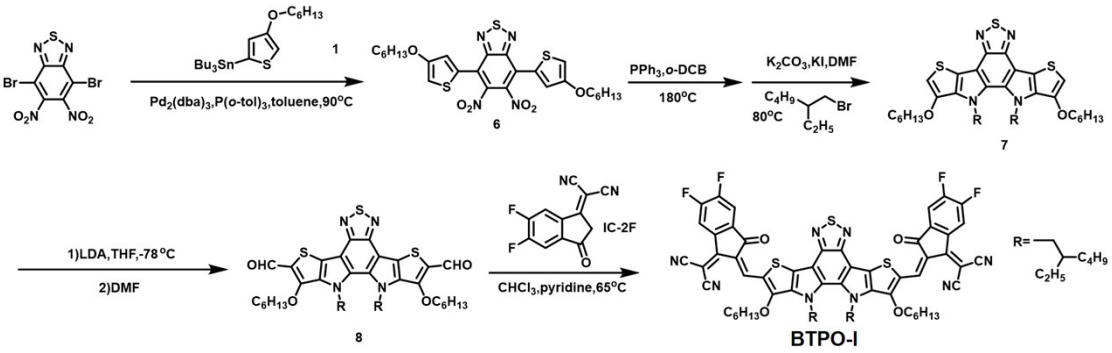

Scheme S2. The synthetic routes of **BTPO-I**.

Synthesis of compound **6**

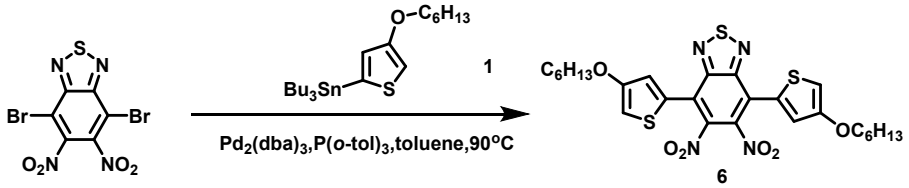

To a solution of 4,7-dibromo-5,6-dinitrobenzo[c][1,2,5]thiadiazole (200.0 mg, 0.521 mmol), $Pd_2(dba)_3$ (23.8 mg, 0.0260 mmol) and P(*o*-tol)$_3$ (63.4 mg, 0.208 mmol) in toluene (10 mL), compound **1** (591.9 mg, 1.25 mmol) was added under N_2. The reaction mixture was stirred for 12 hours at 90 °C. Then, the reaction mixture was cooled to room temperature and poured into an aqueous potassium fluoride. The mixture was extracted with ethyl acetate for three times. The combined organic phase was washed with water followed by brine. Then the solution was dried over Na_2SO_4 and concentrated under reduced pressure. The residue was purified by flash column chromatography (eluent: *n*-hexane: CH_2Cl_2= 2:1, v/v) to get the product as dark red oil (187.0 mg, 61%).^{1}H NMR (400 MHz, $CDCl_3$, ppm): δ= 7.17 (d, 2H, *J*= 4.0 Hz), 6.64 (d, 2H, *J*= 4.0 Hz), 3.98 (t, 4H, *J*= 6.0 Hz) , 1.81-1.77 (m, 6H), 1.48-1.35 (m, 10H), 0.93-0.90 (m, 6H); ^{13}C NMR (100 MHz, $CDCl_3$, ppm): δ= 158.1, 152.2, 141.8, 128.2, 123.2, 121.5, 103.9, 70.7, 31.7, 29.3, 25.9, 22.8, 14.2. MALDI-TOF MS: calcd for

$C_{26}H_{30}N_4O_6S_4$ (M^+), 590.1327; found, 590.0985.

Synthesis of compound **7**

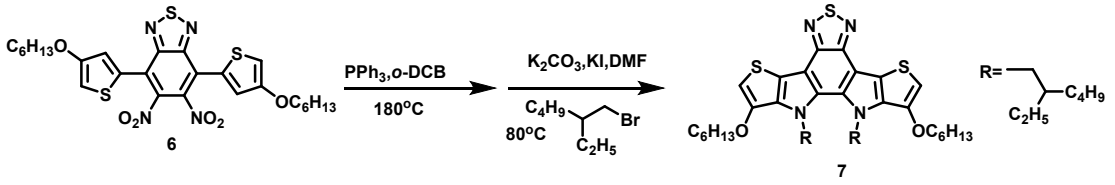

Compound **6** (197.2 mg, 0.3262 mmol) and PPh_3 (855.1 mg, 3.26 mmol) were dissolved in the 1,2-dichlorobenzene (*o*-DCB, 10 mL) under nitrogen. After being heated at 180 °C for 3 hrs, the solvent was removed to get the crude product.

The red residue was mixed with 3-(bromomethyl)heptane (1.510 g, 7.83 mmol), potassium carbonate (900.8 mg, 6.52 mmol) and potassium iodide (1.298 g, 7.83 mmol) in DMF (10 mL) under N_2. The mixture was refluxed at 80 °C overnight. After cooled down to room temperature, the residue was poured into water and extracted with ethyl acetate three times. The combined organic phase was washed with water followed by brine. Then the solution was dried over Na_2SO_4 and concentrated under reduced pressure. The residue was purified by flash column chromatography (eluent: *n*-hexane: CH_2Cl_2= 3:1, v/v) to get the product as orange oil (56 mg, 23%). ^{1}H NMR (400 MHz, $CDCl_3$, ppm): δ= 6.31 (s, 2H), 4.60 (m, 4H), 4.16 (t, 4H, *J*= 6.0 Hz), 1.93-1.86 (m, 6H), 1.62-1.26 (m, 14H), 1.02-0.57 (m, 32H); ^{13}C NMR (100 MHz, $CDCl_3$, ppm): δ= 148.0, 144.9, 134.9, 133.9, 120.5, 111.0, 98.0, 70.7, 53.5, 40.5, 31.8, 29.7, 29.6, 26.2, 23.0, 22.9, 14.3, 14.0. MALDI-TOF MS: calcd for $C_{42}H_{62}N_4O_2S_3$, 750.4035; found, 750.4221.

Synthesis of compound **8**

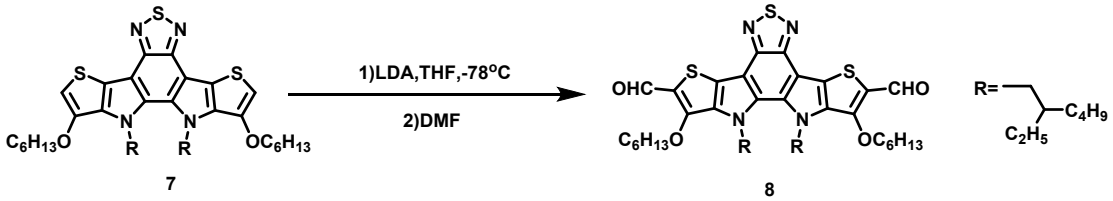

7 8

To a solution of compound **7** (56 mg, 0.0694 mmol) in THF (10 mL), 2.0 M lithium diisopropylamide in hexane (0.28 mL, 0.556 mmol) was added dropwise slowly at −78 °C under N_2. The mixture was stirred at −78 °C for 1 h, and then anhydrous DMF (0.28 mL) was added. The mixture was stirred overnight at room temperature. Brine was added and the mixture was extracted with ethyl acetate for three times. The combined organic phase was washed with water followed by brine. Then the solution was dried over Na_2SO_4 and concentrated under reduced pressure. The residue was purified by flash column chromatography (eluent: CH_2Cl_2) to get the product as orange solid (50.0 mg, 89%).^{1}H NMR (400 MHz, $CDCl_3$, ppm): δ= 10.19 (s, 2H), 4.54-4.50 (m, 8H), 1.99-1.84 (m, 6H), 1.60-1.2 (m, 14H), 1.00-0.61 (m, 32H); ^{13}C NMR (100 MHz, $CDCl_3$, ppm): δ= 181.6, 150.2, 136.2, 136.1, 127.8, 124.6, 123.7, 112.7, 77.7, 53.9, 40.7, 31.7, 31.7, 30.4, 30.4, 30.3, 29.9, 25.8, 23.0, 22.8, 14.3, 14.0.MALDI-TOF MS: calcd for $C_{44}H_{62}N_4O_4S_3$ (M^+), 806.3933; found, 806.4372.

Synthesis of **BTPO-l**

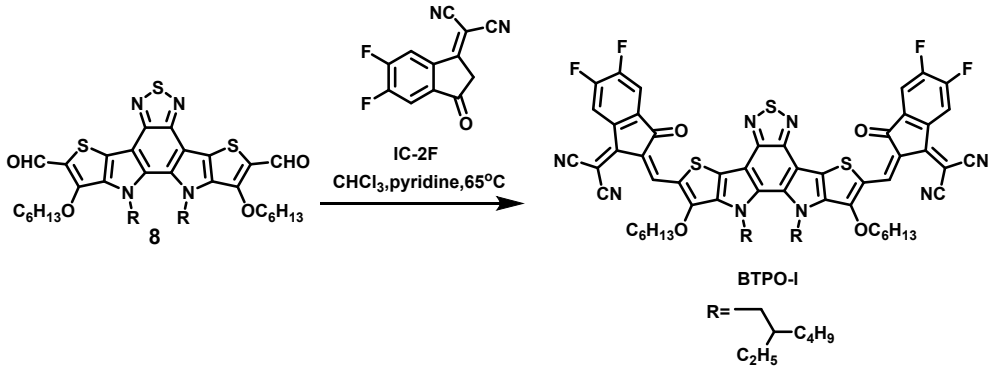

8

To a solution of compound **8** (50.0 mg, 0.0620 mmol) and 2-(5, 6-dichloro-3-oxo-

2,3-dihydro-1*H*-inden-1-ylidene) malononitrile (**IC-2F**) (85.6 mg, 0.372 mmol) in dry $CHCl_3$ (10 mL) was added pyridine (1 mL) under N_2. The mixture was refluxed for 16 hours and then allowed to cool to room temperature, then the mixture was poured into CH_3OH (100 mL) and filtered, the residue left in filter paper was dissolved by $CHCl_3$. After removing the solvent, the residue was purified using column chromatography on silica gel (eluent: *n*-hexane: CH_2Cl_2= 1:1 , v/v), yielding a dark purple solid (41.0 mg, 54%).^{1}H NMR (400 MHz, $CDCl_3$, ppm): δ= 9.21 (s, 2H), 8.53-8.49 (m, 2H), 7.69-7.65 (m, 2H), 4.61-4.59 (m, 4H), 4.42 (t, 4H, *J*= 8.0 Hz), 2.10-1.96 (m, 6H), 1.54-1.25 (m, 14H), 1.06-0.64 (m, 32H); Note that the ^{13}C NMR spectrum cannot be obtained because BTPO-l easily crystallized out from the solution during the test. Actually, we tried the ^{13}C NMR measurement overnight for three times. However, no signal was detected. MALDI-TOF MS: calcd for $C_{68}H_{66}F_4N_8O_4S_3$ (M^+), 1230.4305; found, 1230.4214.

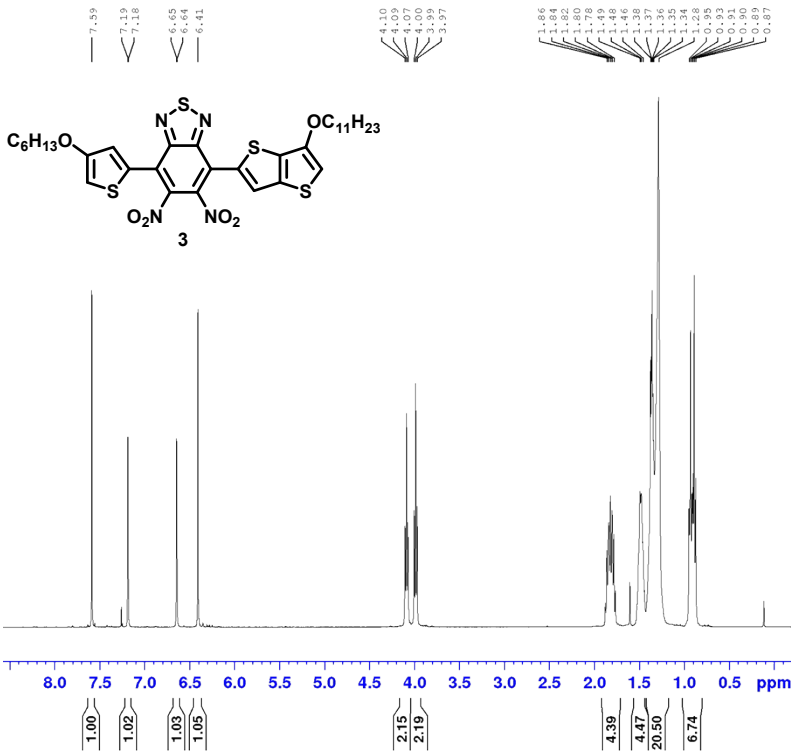

Figure S10 ^{1}HNMR spectrum of compound **3** (400 MHz, $CDCl_3$).

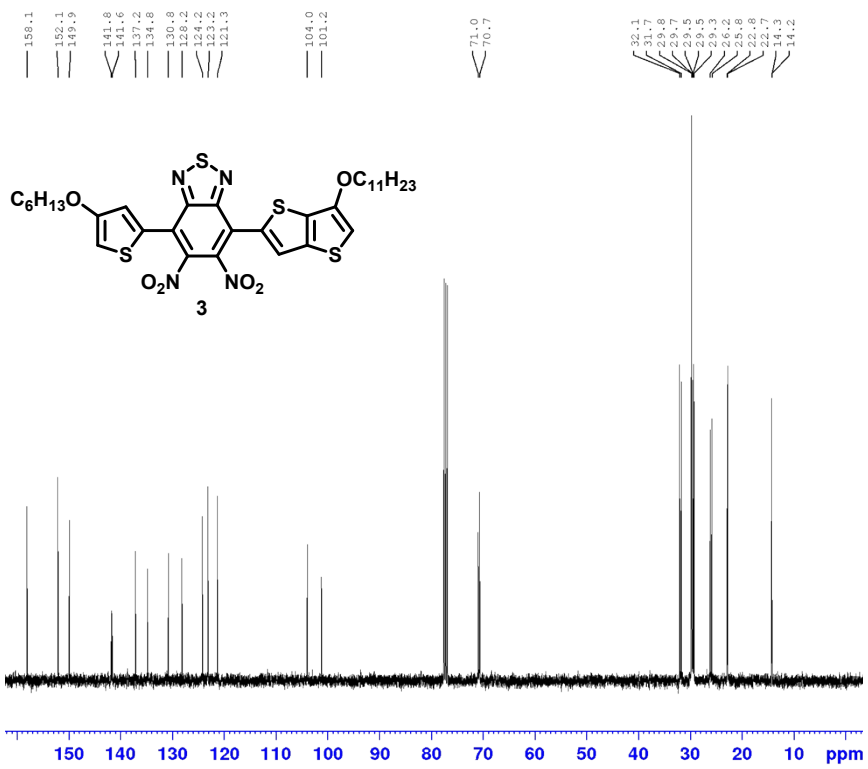

Figure S11 ^{13}CNMR spectrum of compound **3** (100 MHz, $CDCl_3$).

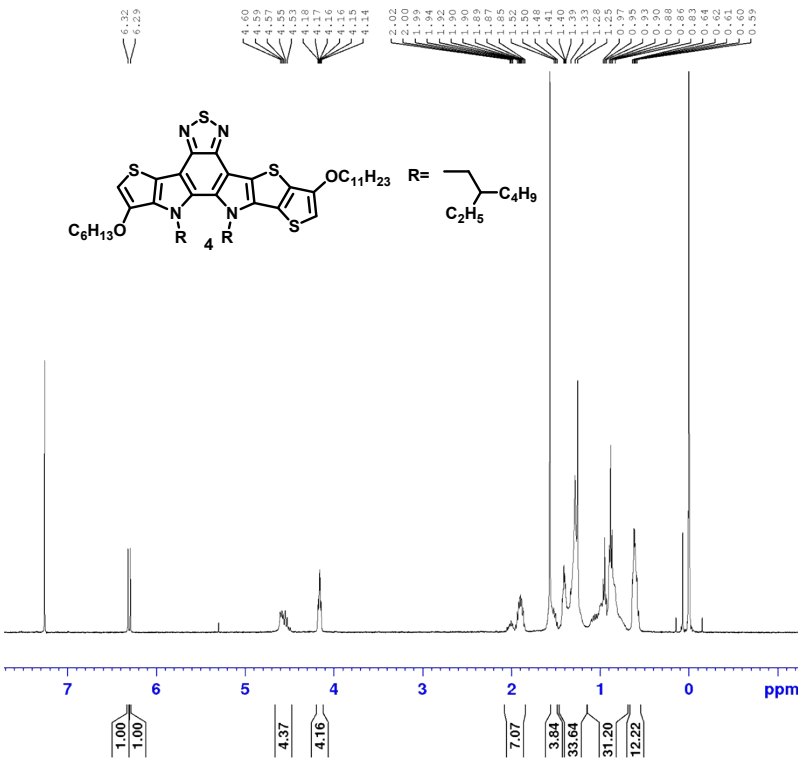

Figure S12 ^{1}HNMR spectrum of compound **4** (400 MHz, $CDCl_3$).

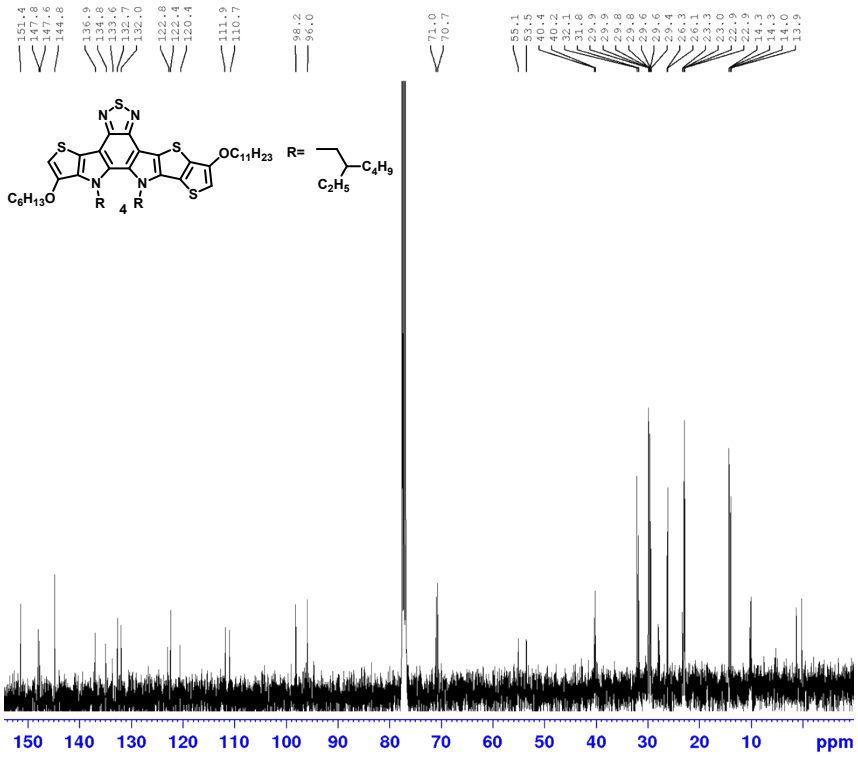

Figure S13 ^{13}CNMR spectrum of compound **4** (100 MHz, $CDCl_3$).

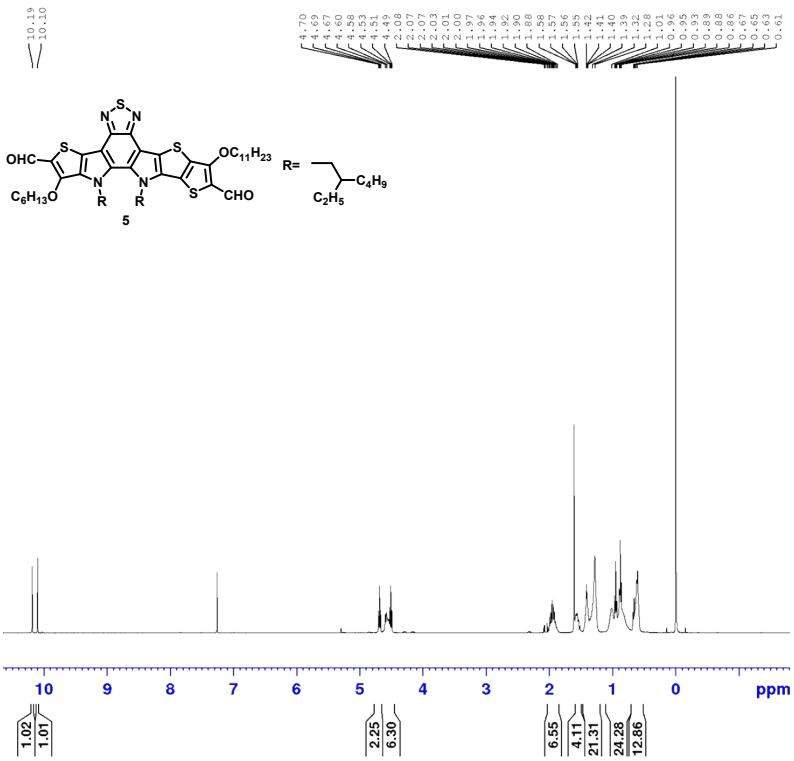

Figure S14 ^{1}HNMR spectrum of compound **5** (400 MHz, $CDCl_3$).

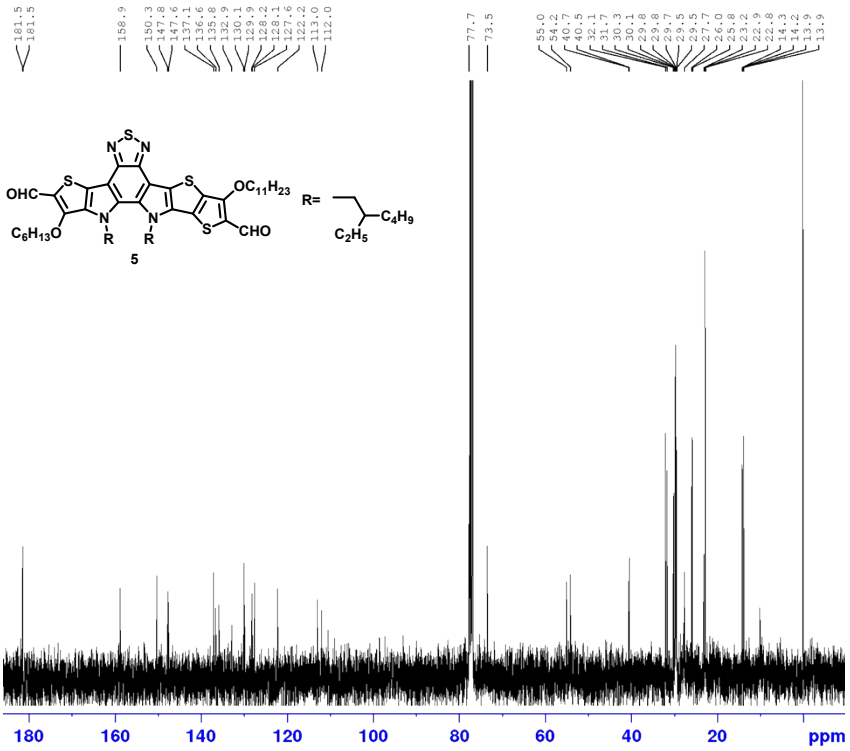

Figure S15 ^{13}CNMR spectrum of compound **5** (100 MHz, $CDCl_3$).

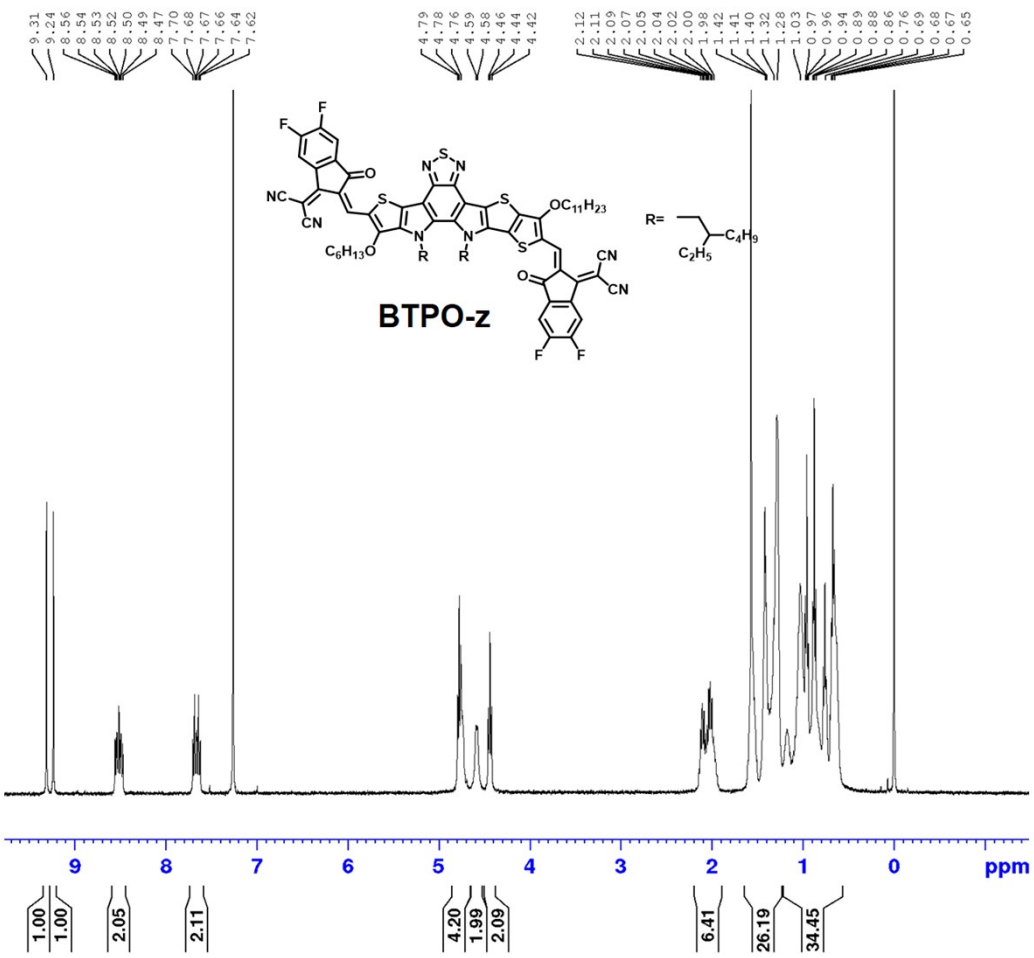

Figure S16 ^{1}HNMR spectrum of **BTPO-z** (400 MHz, $CDCl_3$).

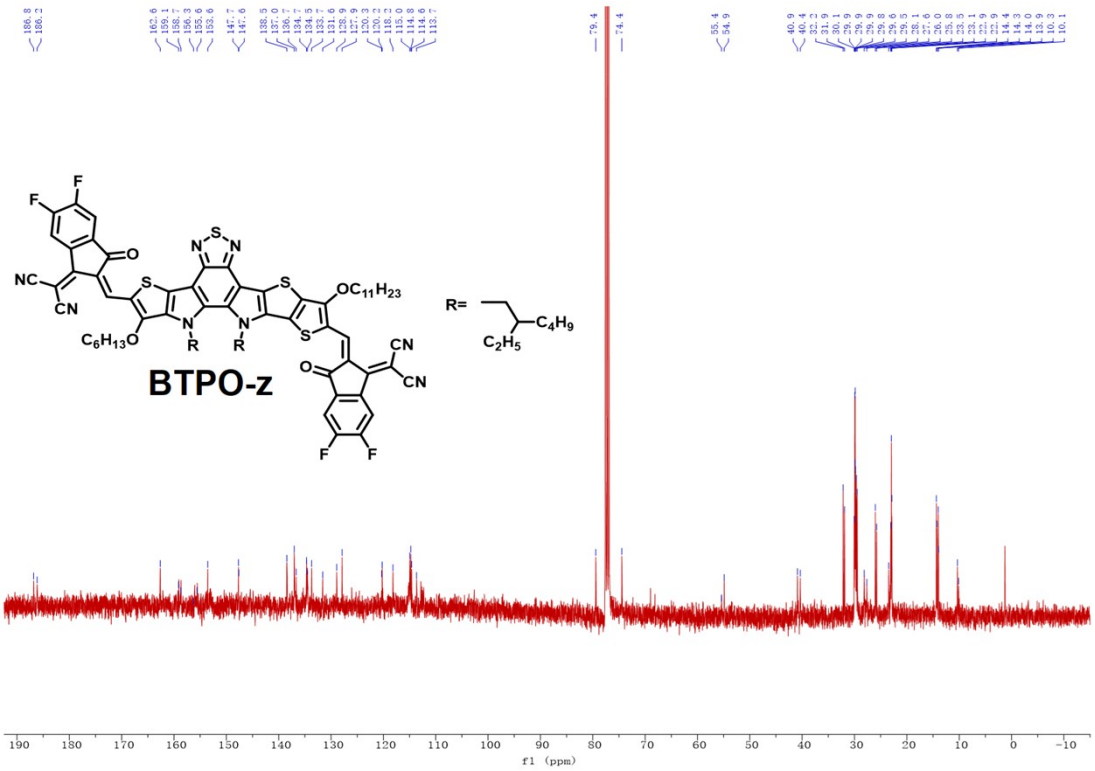

Figure S17 ^{13}CNMR spectrum of **BTPO-z** (100 MHz, $CDCl_3$).

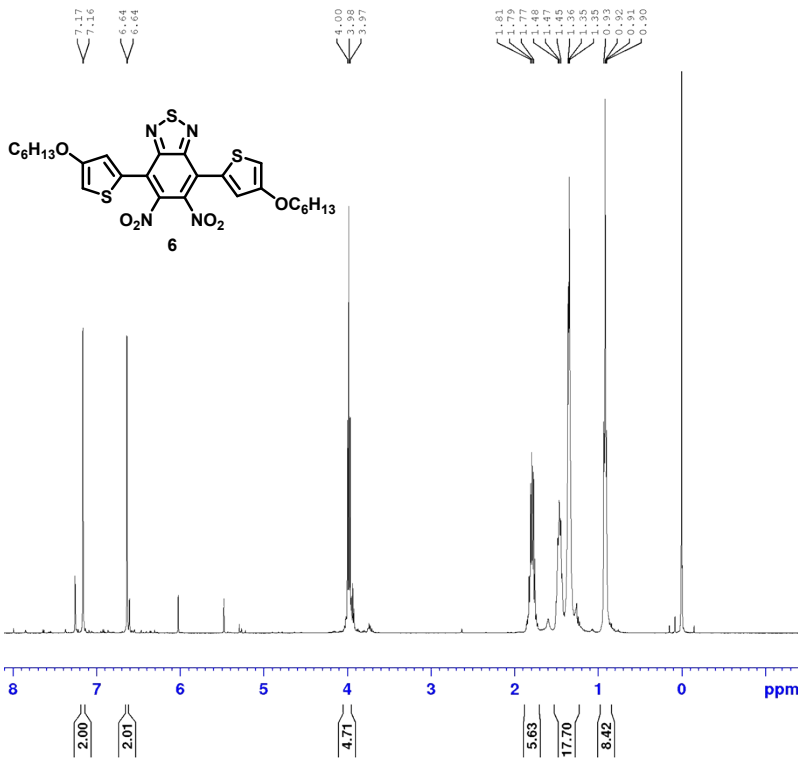

Figure S18 ^{1}HNMR spectrum of compound **6** (400 MHz, $CDCl_3$).

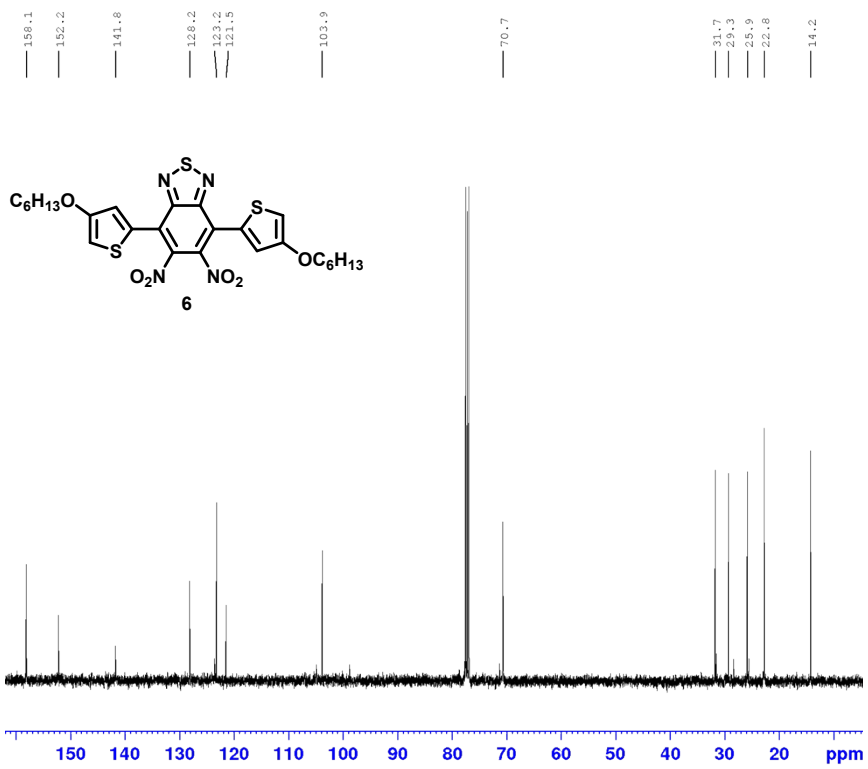

Figure S19 ^{13}CNMR spectrum of compound **6** (100 MHz, $CDCl_3$).

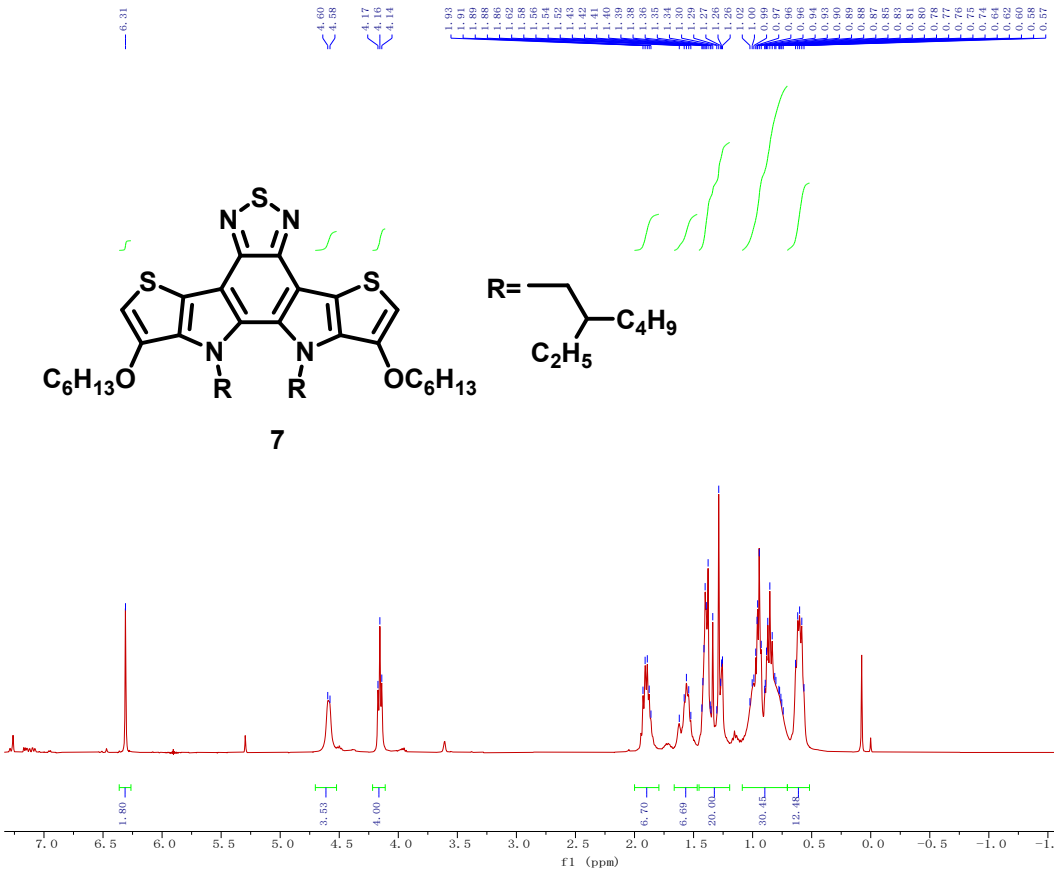

Figure S20 ^{1}HNMR spectrum of compound **7** (400 MHz, $CDCl_3$).

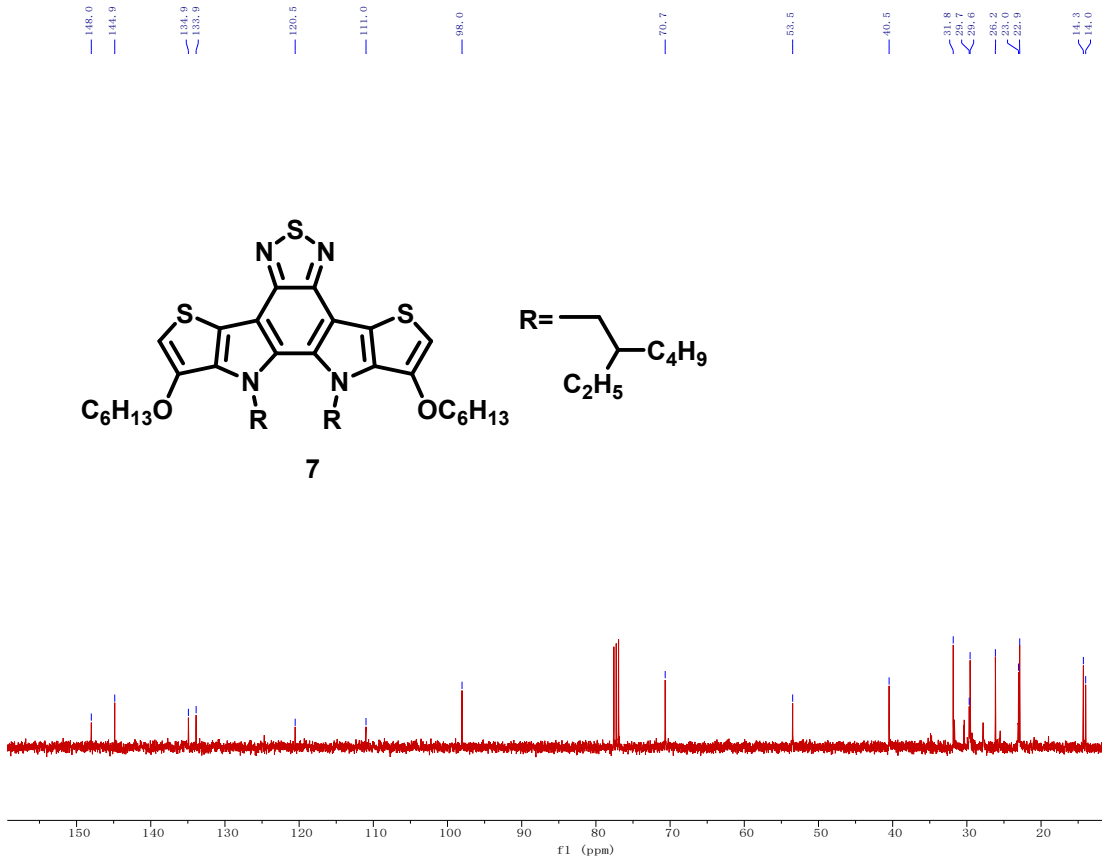

Figure S21 ^{13}CNMR spectrum of compound **7** (100 MHz, $CDCl_3$).

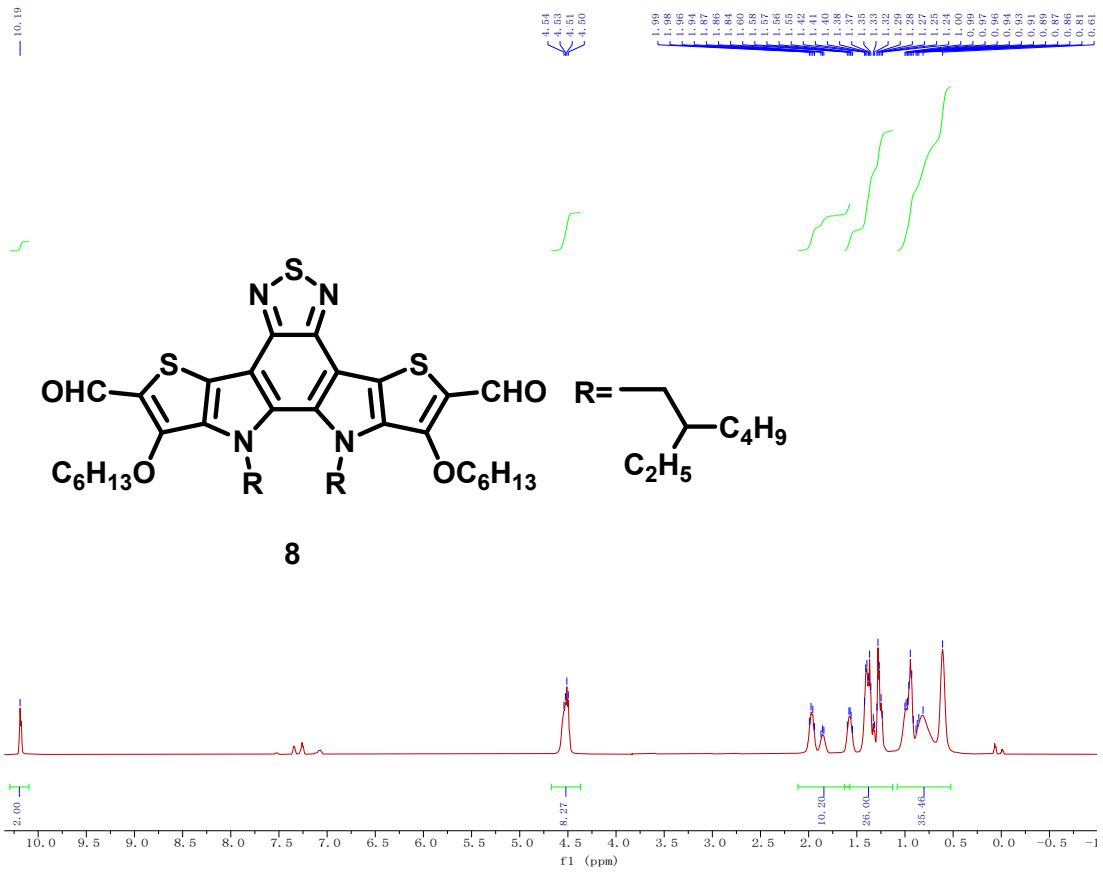

Figure S22 ^{1}HNMR spectrum of compound **8** (400 MHz, $CDCl_3$).

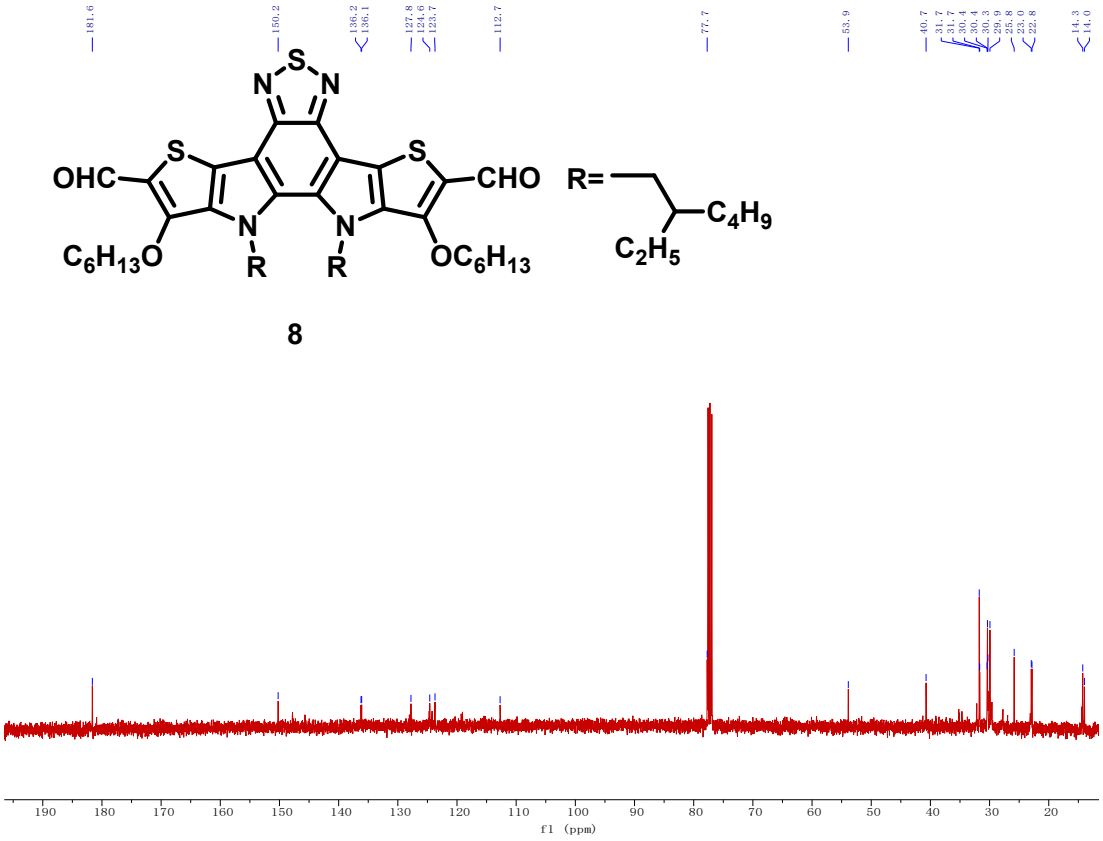

Figure S23 ^{13}CNMR spectrum of compound **8** (100 MHz, $CDCl_3$).

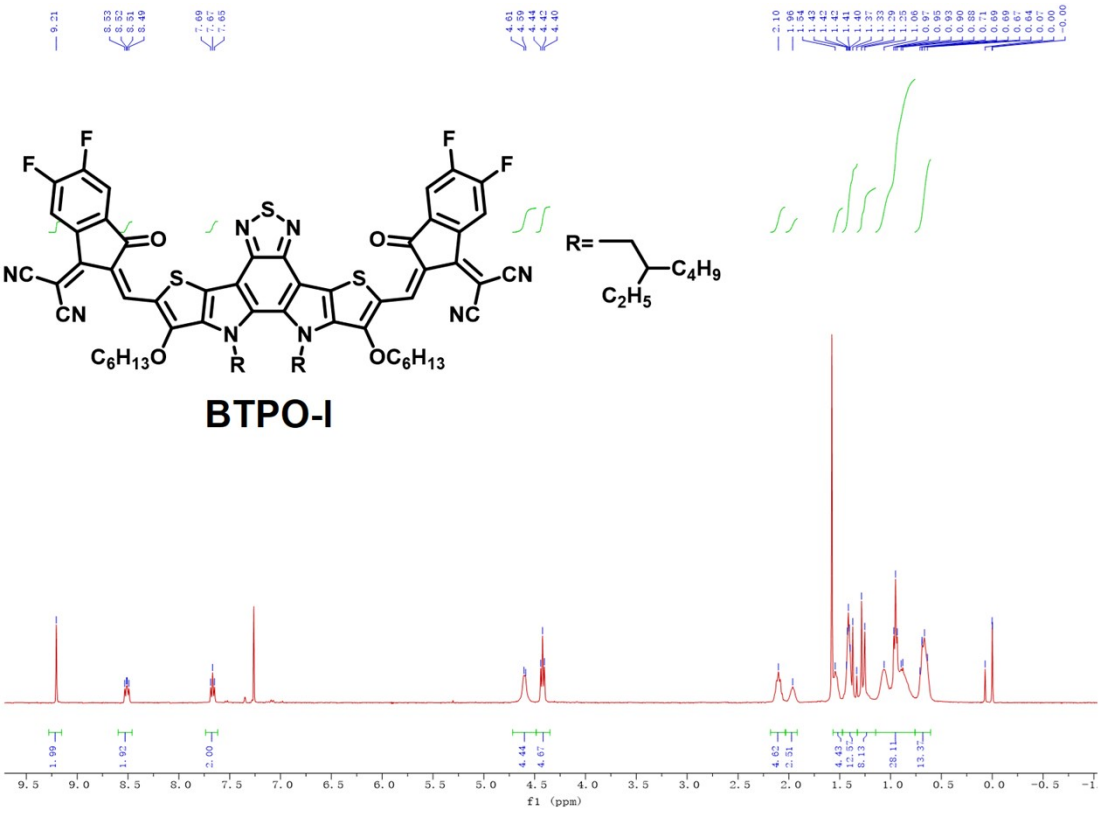

Figure S24 ^{1}HNMR spectrum of BTPO-l (400 MHz, $CDCl_3$).

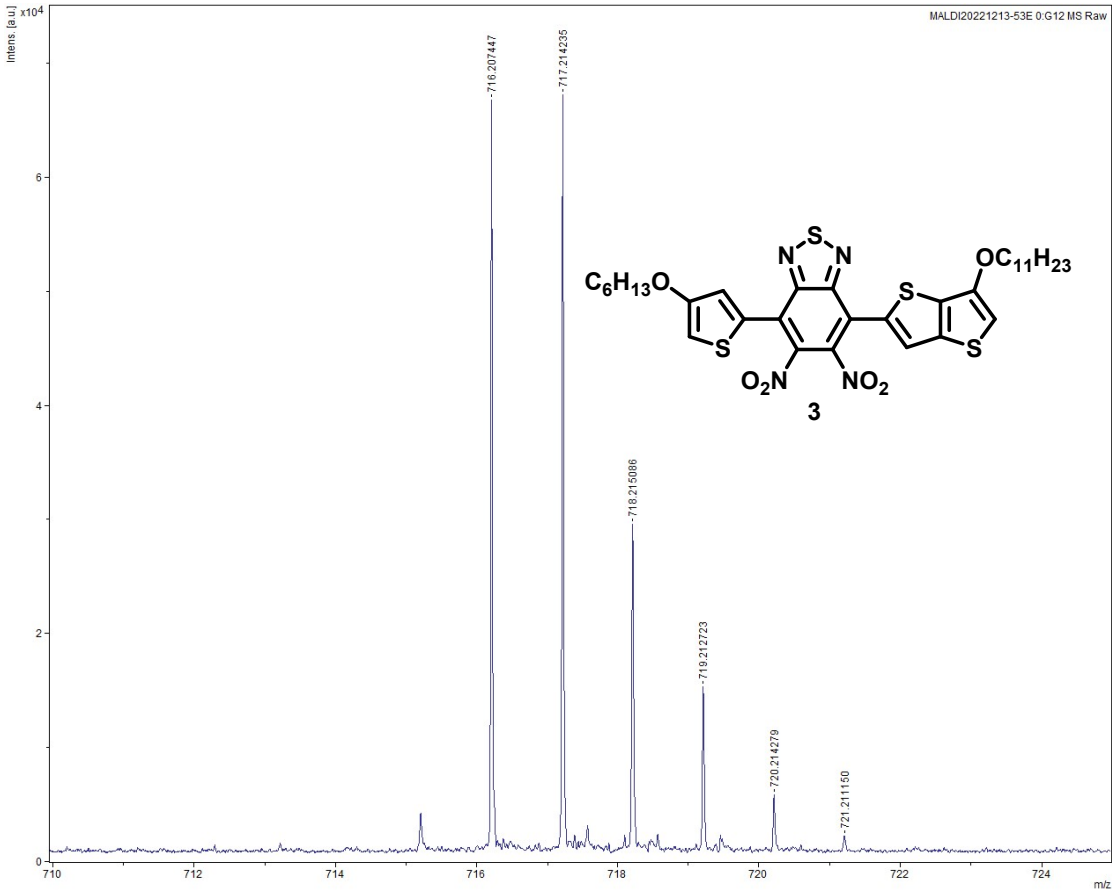

Figure S25. MS spectrum (MALDI-TOF) of compound **3**.

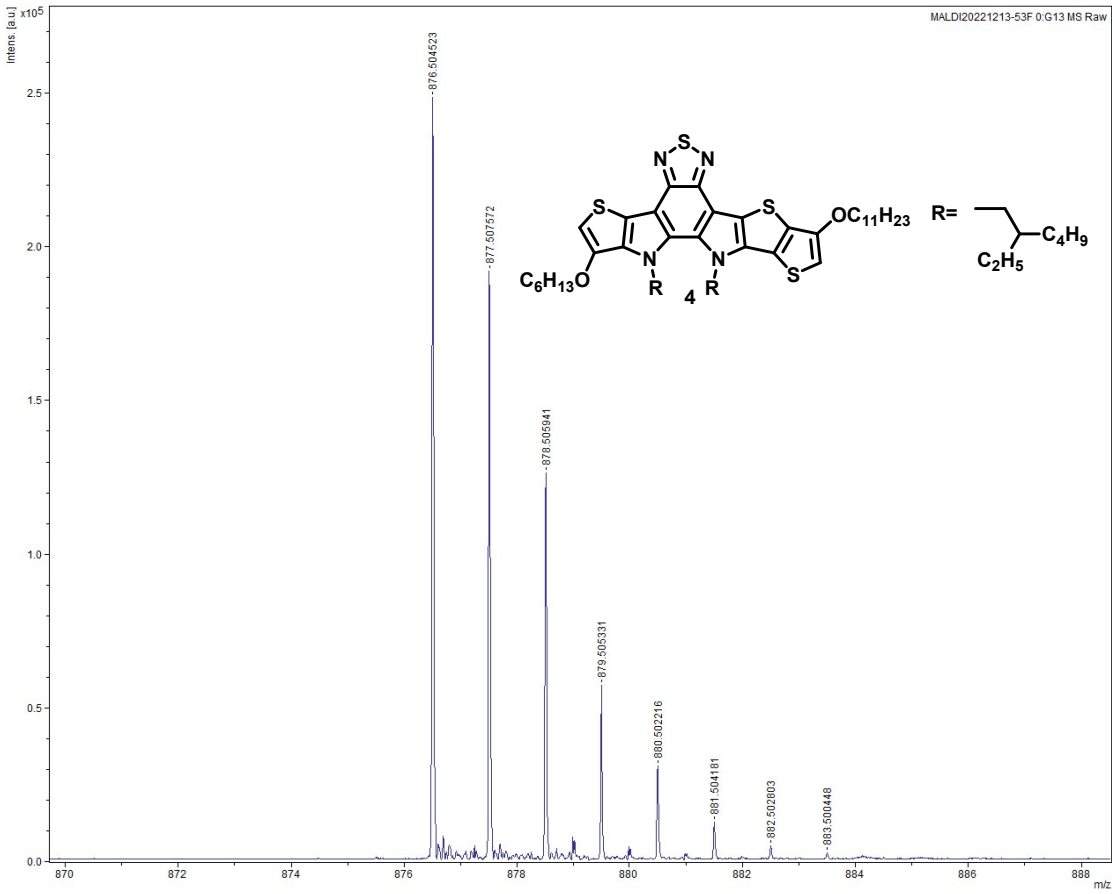

Figure S26. MS spectrum (MALDI-TOF) of compound **4**.

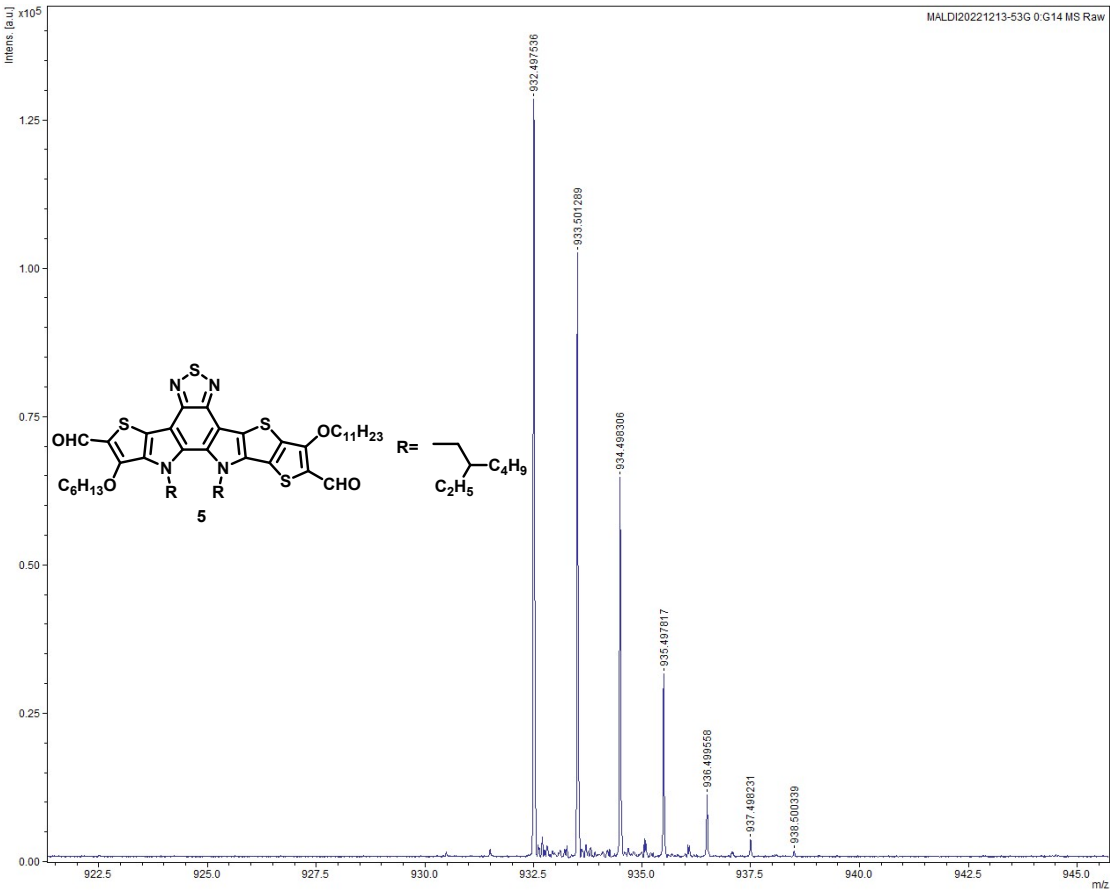

Figure S27. MS spectrum (MALDI-TOF) of compound **5**.

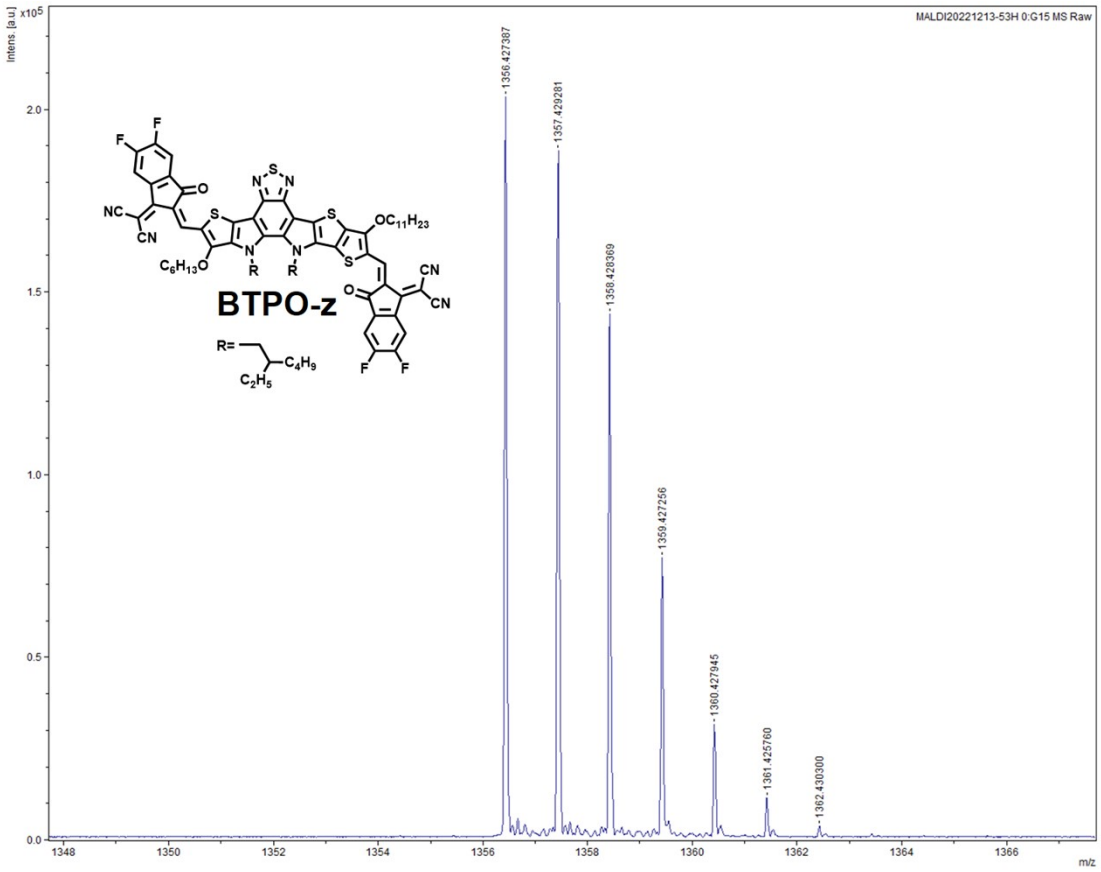

Figure S28. MS spectrum (MALDI-TOF) of **BTPO-z**.

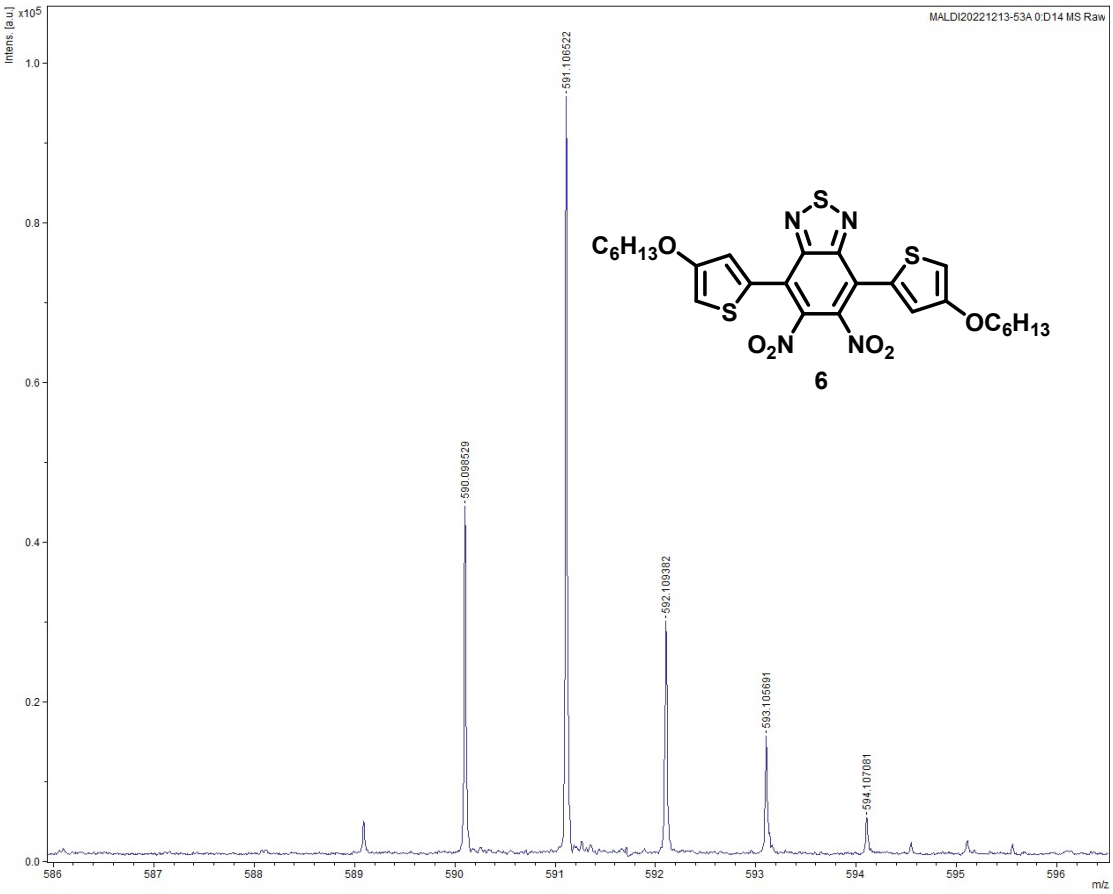

Figure S29. MS spectrum (MALDI-TOF) of compound **6**.

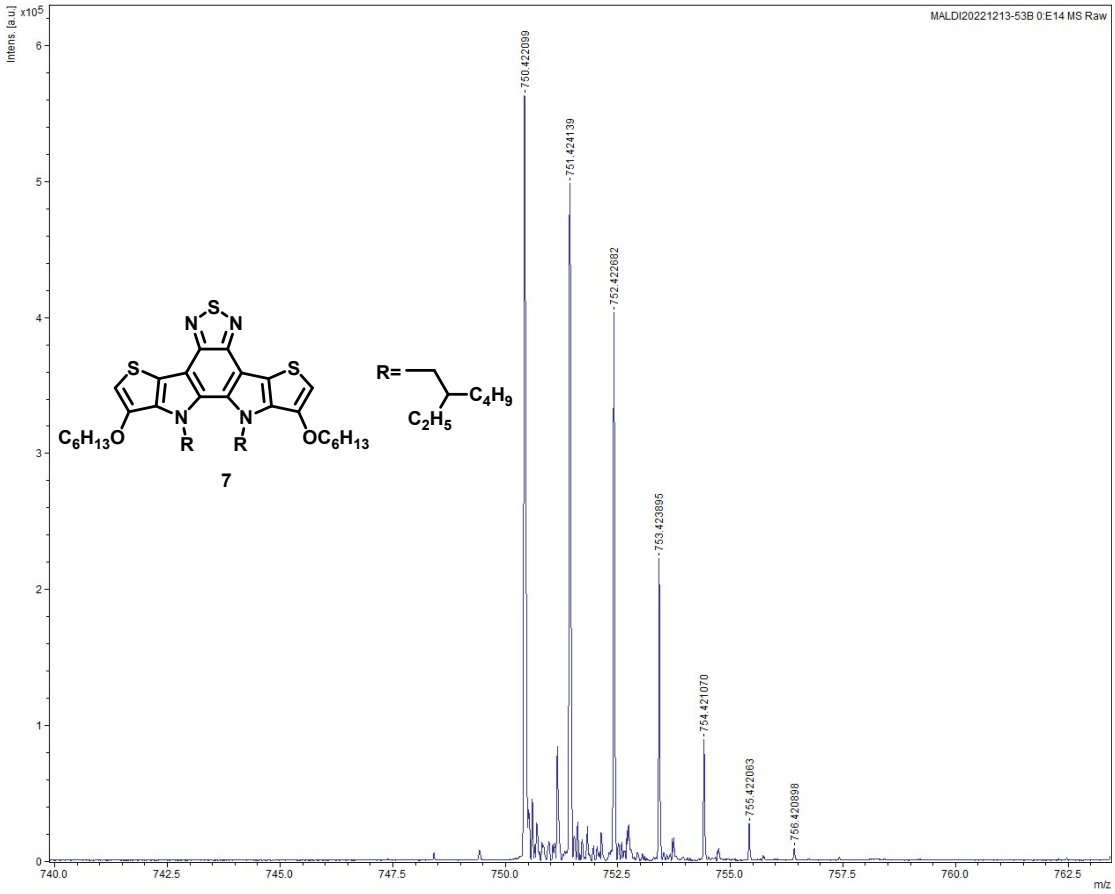

Figure S30. MS spectrum (MALDI-TOF) of compound **7**.

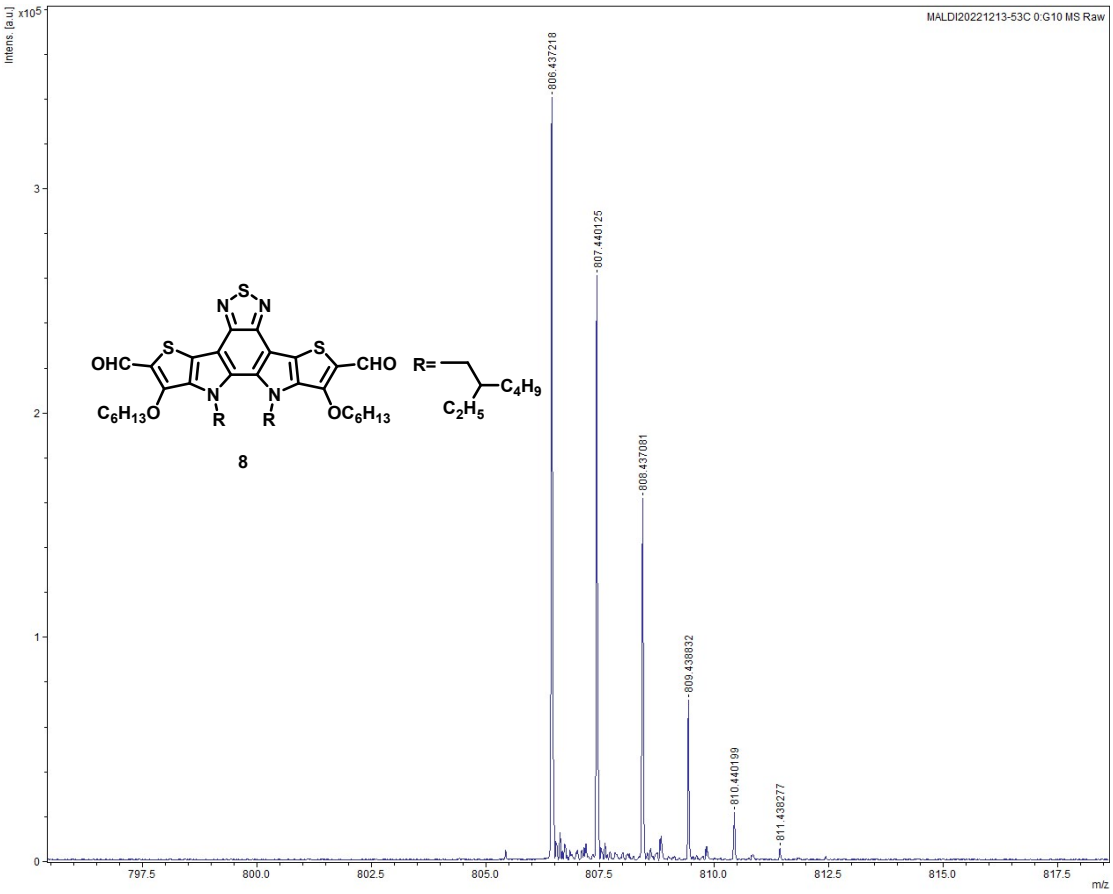

Figure S31. MS spectrum (MALDI-TOF) of compound **8**.

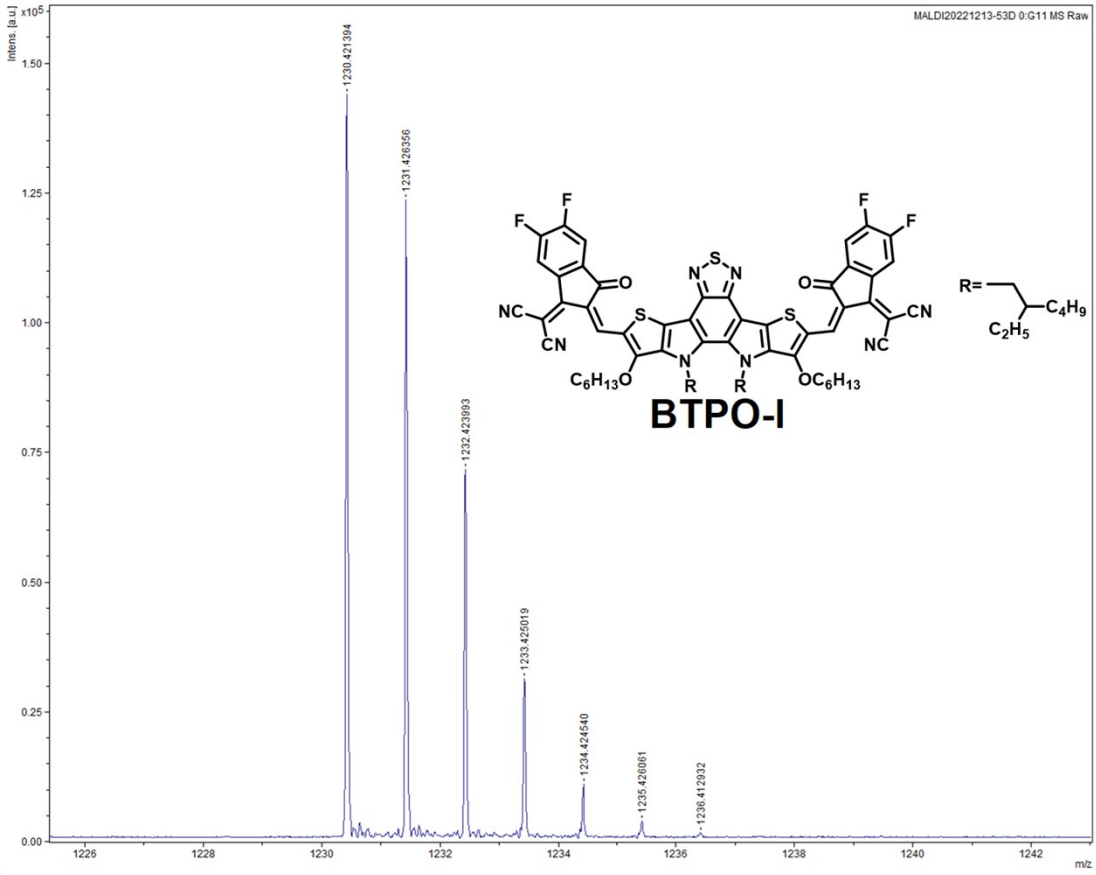

Figure S32. MS spectrum (MALDI-TOF) of **BTPO-l**.

Reference

[1] Y. Chen, F. Bai, Z. Peng, L. Zhu, J. Zhang, X. Zou, Y. Qin, H. K. Kim, J. Yuan, L.-K. Ma, J. Zhang, H. Yu, P. C. Y. Chow, F. Huang, Y. Zou, H. Ade, F. Liu, H. Yan, *Adv. Energy Mater.* **2021**, *11*, 2003141.

[2] Y. Zhang, X. Liu, M. Wang, X. Liu, J. Zhao, in *Polymers*, Vol. 8, 2016.

[3] M. J. Frisch, G. W. Trucks, H. B. Schlegel, G. E. Scuseria, M. A. Robb, J. R. Cheeseman, G. Scalmani, V. Barone, G. A. Petersson, H. Nakatsuji, X. Li, M. Caricato, A. V. Marenich, J. Bloino, B. G. Janesko, R. Gomperts, B. Mennucci, H. P. Hratchian, J. V. Ortiz, A. F. Izmaylov, J. L. Sonnenberg, Williams, F. Ding, F. Lipparini, F. Egidi, J. Goings, B. Peng, A. Petrone, T. Henderson, D. Ranasinghe, V. G. Zakrzewski, J. Gao, N. Rega, G. Zheng, W. Liang, M. Hada, M. Ehara, K. Toyota, R. Fukuda, J. Hasegawa, M. Ishida, T. Nakajima, Y. Honda, O. Kitao, H. Nakai, T. Vreven, K. Throssell, J. A. Montgomery Jr., J. E. Peralta, F. Ogliaro, M. J. Bearpark, J. J. Heyd, E. N. Brothers, K. N. Kudin, V. N. Staroverov, T. A. Keith, R. Kobayashi, J. Normand, K. Raghavachari, A. P. Rendell, J. C. Burant, S. S. Iyengar, J. Tomasi, M. Cossi, J. M. Millam, M. Klene, C. Adamo, R. Cammi, J. W. Ochterski, R. L. Martin, K. Morokuma, O. Farkas, J. B. Foresman, D. J. Fox, Wallingford, CT 2016.

[4] R. A. Marcus, *J. Chem. Phys* **2004**, *24*, 966.

[5] N. S. Hush, *J. Chem. Phys* **2004**, *28*, 962.

[6] J. J. Kwiatkowski, J. Nelson, H. Li, J. L. Bredas, W. Wenzel, C. Lennartz, *Phys. Chem. Chem. Phys.* **2008**, *10*, 1852.

[7] M. Pavanello, J. Neugebauer, *J. Chem. Phys* **2011**, *135*, 234103.

[8] B. Balambiga, P. Devibala, D. Harshini, P. M. Imran, S. Nagarajan, *Mater. Chem. Front.* **2023**, *7*, 2225.

[9] S. Wen, W.-Q. Deng, K.-L. Han, *Chem. Commun. (Camb.)* **2010**, *46*, 5133.

[10] S. Ya-Rui, W. Hui-Ling, S. Ya-Ting, L. Yu-Fang, *CrystEngComm* **2017**, *19*, 6008.

[11] V. T. T. Huong, T. B. Tai, M. T. Nguyen, *J. Phys. Chem. A* **2014**, *118*, 3335.

[12] R. V. Ambili, D. Sasikumar, P. Hridya, M. Hariharan, *Chem. Eur. J.* **2019**, *25*, 1992.

[13] Y. Chen, Z. Wu, L. Ding, S. Zhang, Z. Chen, W. Li, Y. Zhao, Y. Wang, Y. Liu, *Adv. Funct. Mater.* **2023**, *33*, 2304316.

[14] W.-Q. Deng, L. Sun, J.-D. Huang, S. Chai, S.-H. Wen, K.-L. Han, *Nat. Protoc.* **2015**, *10*, 632.

[15] A. Mahmood, J.-L. Wang, *Solar RRL* **2020**, *4*, 2000337.

[16] F. Lin, K. Jiang, W. Kaminsky, Z. Zhu, A. K. Y. Jen, *J. Am. Chem. Soc.* **2020**, *142*, 15246.

[17] B. Spingler, S. Schnidrig, T. Todorova, F. Wild, *CrystEngComm* **2012**, *14*, 751.

[18] H. Jiang, C. Kloc, *MRS Bull.* **2013**, *38*, 28.

[19] G. Zhao, H. Dong, Q. Liao, J. Jiang, Y. Luo, H. Fu, W. Hu, *Nat. Commun.* **2018**, *9*, 4790.